Synthesis of linked carbon monolayers: Films, balloons, tubes, and pleated sheets

Mitchell J. Schultz*†, Xiaoyu Zhang*‡, Sakulsuk Unarunotai*†, Dahl-Young Khang*‡, Qing Cao*†, Congjun Wang*‡, Changhui Lei*‡, Scott MacLaren*‡, Julio A. N. T. Soares*†, Ivan Petrov*‡, Jeffrey S. Moore*†‡§, and John A. Rogers*†‡§¶‖

*Frederick Seitz Materials Research Laboratory, Departments of †Chemistry, ‡Materials Science and Engineering, ¶Mechanical Science and Engineering, and ‖Electrical and Computer Engineering, University of Illinois at Urbana-Champaign, Urbana, IL 61801

Edited by Uwe Bunz, Carnegie Mellon University, and accepted by the Editorial Board March 26, 2008 (received for review October 23, 2007)

Because of their potential for use in advanced electronic, nanomechanical, and other applications, large two-dimensional, carbon-rich networks have become an important target to the scientific community. Current methods for the synthesis of these materials have many limitations including lack of molecular-level control and poor diversity. Here, we present a method for the synthesis of two-dimensional carbon nanomaterials synthesized by Mo- and Cu-catalyzed cross-linking of alkyne-containing self-assembled monolayers on SiO_2 and Si_3N_4. When deposited and cross-linked on flat surfaces, spheres, cylinders, or textured substrates, monolayers take the form of these templates and retain their structure on template removal. These nanomaterials can also be transferred from surface to surface and suspended over cavities without tearing. This approach to the synthesis of monolayer carbon networks greatly expands the chemistry, morphology, and size of carbon films accessible for analysis and device applications.

networks | nanomaterials | self-assembled

In contrast to carbon nanotubes, fullerenes and various derivatives (1–3), the synthesis of large 2D sheets such as graphene (4), graphyne, and graphdiyne (5, 6) extending over micrometers in lateral dimensions is either in its infancy or has significant limitations. In fact, the synthesis of 2D carbon networks has been recognized as an outstanding challenge in materials chemistry (7).

Graphene, the simplest of the 2D conjugated carbon nanomaterials, is produced by micromechanical cleavage of bulk graphite (HOPG) or by thermal decomposition of silicon carbide (8, 9). However, these approaches lack the molecular-level control necessary to define the chemical makeup of these systems. Scholl coupling reactions on oligophenylene precursors (10) produce small (<15 nm) 2D graphene fragments with improved molecular diversity, and radiation induced modifications of self-assembled (11, 12) or Langmuir–Blodgett (13) monolayers create larger sheets, but with reduced control of the chemistry. Polyelectrolytes (14) represent a different class of chemistry that can form 2D (15) and 3D (16) nanomaterials. These films are formed through deposition of separately synthesized polymers, often in layer-by-layer assemblies, in the form of relatively thick (typically >5 nm) films governed by electrostatic interactions. These limitations, together with those associated with the planar, radiation-cross-linked monolayers, motivate the need for alternative approaches to these classes of materials.

A potential solution to the formation of large 2D conjugated carbon nanomaterials would employ a two-step procedure involving the formation of self-assembled monolayers (SAMs) with highly functionalized monomers followed by chemical cross-linkage of the SAMs to form linked monolayers. Fig. 1 shows the overall process beginning with the formation of SAMs of suitably designed carbon precursors on solid supports, followed by chemical cross-linking to yield covalently bonded networks with monolayer thicknesses. Not only could these materials adopt the geometry of the support, but they could also be transferred by using printing-like techniques to other substrates or lithographically patterned into desired geometries. This article introduces the use of synthetic organic methods to create linked carbon monolayers and monolayer membranes in forms ranging from planar or structured films and membranes, to spherical coatings, balloons, tubes, and other complex topologies.

Results

Aryl alkynes are attractive monomers for this chemistry because they are a chemically diverse class of molecules that are already highly conjugated, contain primarily carbon by mass, and can be chemically linked through a variety of methods including alkyne metathesis (17), oxidative Cu coupling (18), and Pd-catalyzed cross-coupling (18). Di-functional monomers (**1** and **2**) and a hexa-functional monomer (**3**) were synthesized with triethoxysilyl groups attached by a carbamate group to the aryl core (Fig. 1*B*) [supporting information (SI) *Text*]. SiO_2- or Si_3N_4-coated substrates or quartz/glass slides were immersed in monomer solutions (≈15 mM monomer, ≈10 mM triethylamine, 90–100°C, 24 h, toluene) creating SAMs that exhibited similar advancing contact angles (74–80°) for all three monomers (Table S1). Two different cross-linking chemistries were used to form linked monolayers from these SAMs. Mo(IV)-catalyzed, vacuum-driven alkyne metathesis (17) linked the dipropyne SAMs derived from **1**. Cu-catalyzed Hay-type coupling conditions (18) created linked monolayers from SAMs of monomers **2** and **3**. The advancing contact angles consistently decreased by 6, 11, and 20° for the dipropyne (**1**), diacetylene (**2**), and terphenyl (**3**) chemistries, respectively. After exposing the SAMs to the linkage conditions, it was found that very little residual metal remained on the substrate.

UV-visible (UV-vis) absorption spectra of the SAMs on UV-grade fused quartz closely matched spectral features of the monomers in solution (Fig. S1). The linked monolayer of **1** on quartz possesses a new shoulder at 330 nm (Fig. 2*A*). Because this new shoulder is small it suggests incomplete polymerization or the formation of oligomers (19, 20). Similarly, the linked monolayer from **2** on quartz possesses a broad new peak at 370 nm (Fig. 2*D*) that matches the absorbance of poly(1,4-phenylene-1,3-butadiynylene) derivatives (20, 21). This has been described as a delocalized $\pi \rightarrow \pi^*$ transition in molecules comprised of multiple 1,4-diphenylbutadiyne chromophores (20). The appearance of these lower-energy peaks suggests an increased delocalization of electrons on oligomerization/polymerization resulting from increased conjugation (21). The spectrum of the linked monolayer of **3** is

Author contributions: M.J.S. and X.Z. contributed equally to this work; M.J.S., X.Z., J.S.M., and J.A.R. designed research; M.J.S., X.Z., S.U., D.-Y.K., Q.C., C.W., and C.L. performed research; X.Z., S.M., J.A.N.T.S., and I.P. contributed new reagents/analytic tools; M.J.S., X.Z., S.U., J.S.M., and J.A.R. analyzed data; and M.J.S., X.Z., J.S.M., and J.A.R. wrote the paper.

Conflict of interest statement: A patent has been filed on this work.

This article is a PNAS Direct Submission. U.B. is a guest editor invited by the Editorial Board.

§To whom correspondence may be addressed. E-mail: moore@scs.uiuc.edu or jrogers@uiuc.edu.

This article contains supporting information online at www.pnas.org/cgi/content/full/0710081105/DCSupplemental.

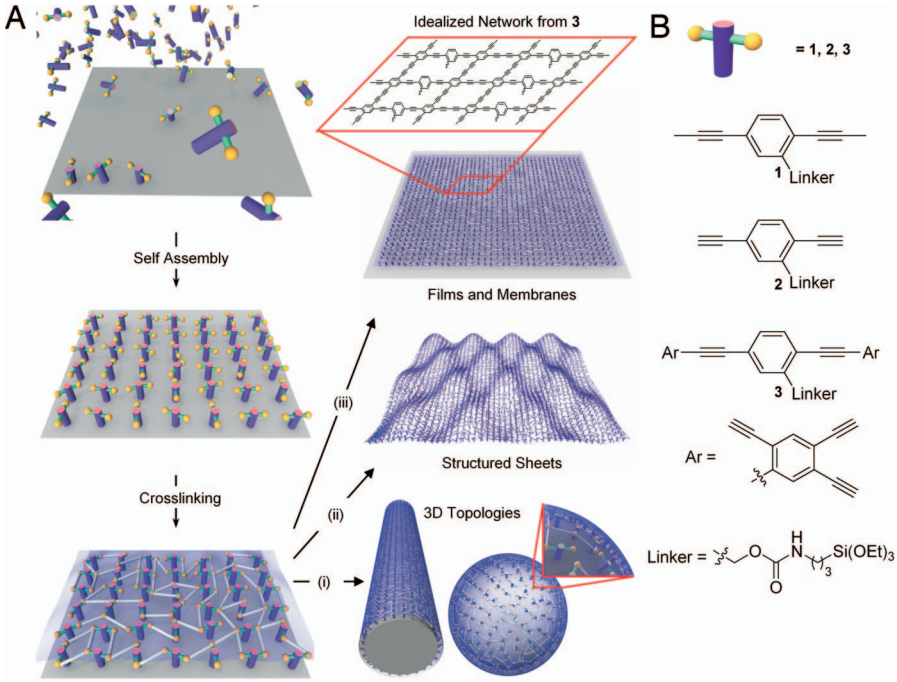

Fig. 1. Schematic illustration of linked monolayer formation. (*A*) Self-assembled monolayers (SAMs) are synthesized on a substrate, then cross-linked to form linked monolayers. This approach is applied to the formation of 3D topologies (*i*), structured sheets (*ii*), and membranes (*iii*). The box above *iii* provides an idealized view of the chemical structure for a linked monomer network formed from monomer 3. (*B*) Chemical structures of monomers 1–3.

significantly broadened compared with that of the original SAM (Fig. S2). No polymers have been synthesized previously from monomers structurally similar to **3**, but the broadening of the absorbance spectra is likely a result of the extensive cross-linking that is possible with this monomer (for an idealized network, see Fig. 1).

Methanol suspensions of SAMs of diacetylene (**2**) coated on 330-nm nonporous SiO_2 spheres exhibit dramatic changes in fluorescence emission on conversion to linked monolayers. A SAM from **2** primarily has a large emission at 315 nm ($\lambda^{ex} = 275$ nm; Fig. 2*E*, blue curves) similar to that of the monomer in solution (Figs. S3–S5). On cross-linking, the emission at 315 nm ($\lambda^{ex} = 275$ nm) weakened significantly and a new emission appeared at 405 nm when excited at 370 nm (Fig. 2*E*, red curves).

Raman spectroscopy provided a convenient means to determine the conversion of SAM **2** to a linked monolayer. Raman spectra of SAM **2** on SiO_2(300 nm)/Si showed a peak at 2,101 cm^{-1}, corresponding to the C≡C stretching mode in terminal phenyl acetylenes (Fig. 2*F*) (22, 23). On exposure of the SAM to cross-linking conditions, the peak at 2,101 cm^{-1} shifts to 2,204 cm^{-1} corresponding to the C≡C stretching mode in phenyl diacetylene (24, 25). The disappearance of the peak from the terminal phenyl acetylene indicates nearly complete conversion of the monomers in the SAM to the corresponding linked monolayer. A variety of conjugated polymers have been previously synthesized that resemble these linked monolayers (20, 21, 26, 27). The spectroscopic changes observed in the monolayer-supported systems are similar to those seen in the literature examples. However, direct comparisons are difficult because the electronics of these polymers are significantly different and very few examples of poly(1,4-phenylene-1,3-butadiynylene) exist (similar to linked SAMs of **2** and **3**). Collectively, the changes in the UV-vis, fluorescence, and Raman spectra provide strong evidence that the SAMs undergo the desired reaction to form linked carbon monolayers Figs. S6 and S7).

In addition to spectroscopic measurements, SAMs and linked monolayers were patterned into 5-μm lines/5-μm space by simple oxygen-reactive ion etching through a layer of photoresist patterned by photolithography. By atomic force micrographs (AFMs), the linked monolayers formed from **1** exhibited only a slight increase in film thickness compared with their SAM precursors (e.g., 1.1–1.4 nm; Fig. 2 *B* and *C*). MM2 molecular geometry optimization of **1** gives a monomer height of ≈1.5 nm, depending on the torsion angle of the aryl rings. The SAM and linked monolayer thicknesses are also similar to those measured for other related system of similar molecular sizes (13, 28). These data indicate that the unlinked and linked SAMs consist of single layers of monomers aligned approximately perpendicular to the surface. The small increase in thickness on cross-linking may be caused by either a change in the orientation of the benzene rings or by the increased average roughness (0.18–0.27 nm). AFM measurements on patterned linked monolayers from **2** and **3** indicate similarly small increases in thickness of 0.5 and 0.3 nm, respectively, relative to their SAMs (Figs. S8–S10). Unlike the films associated with **1**, for which only monolayers form, SAMs from **2** and **3** form multilayers (2.8 and 4.7 nm, respectively) presumably by thermal polymerization during deposition of these reactive multifunctional monomers.

To illustrate the versatility of this approach, we describe methods to release the linked monolayers from their growth substrate and transfer the resulting monolayer membrane to other substrates. These film manipulations made it possible to examine the structural integrity of the monolayer membranes and compare their behavior with the corresponding SAMs. To accomplish this, photoresist is uniformly spin cast onto the SAMs or linked monolayers followed by patterning if desired, and liftoff by selective etching of the support (i.e., bulk SiO_2 or thin films of SiO_2 or Si_3N_4 on other materials) with concentrated HF. The photoresist/SAM or photoresist/monolayer membrane hybrid films are transferred to other substrates and sonicated in acetone to remove the photoresist.

Spectroscopic measurements were performed to examine the possibility of chemical changes in the transferred film induced by exposure to HF, liftoff, and transfer. The UV/vis spectrum of the

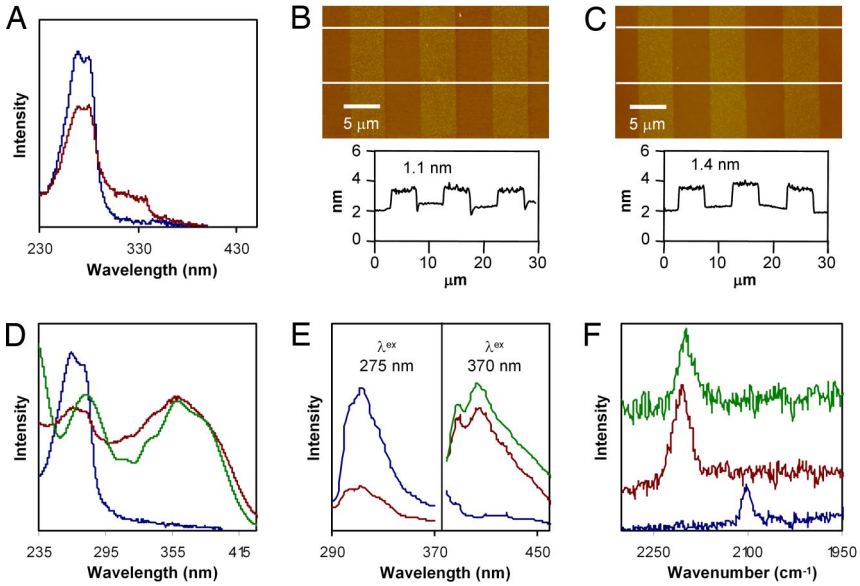

Fig. 2. Spectroscopic data and AFMs of SAMs, linked monolayers, and transferred monolayer membranes. (*A*) Absorption spectra of a SAM (blue), a linked monolayer (red), from **1** on quartz. (*B* and *C*) Tapping-mode AFM of a SAM and a linked monolayer, respectively, from **1** patterned into stripes by photolithography and oxygen-reactive ion etching. The averaged line cuts show a step height of 1.1 nm for the SAM and 1.4 nm for the linked monolayer. (*D*) Absorption spectra of a SAM (blue), a linked monolayer (red), and a transferred monolayer membrane (green) from **2** on quartz. (*E*) Fluorescence spectra (λ^{ex} = 275 nm, *Left*; λ^{ex} = 370 nm, *Right*) of a SAM (blue curves), a linked monolayer (red curves), and an etched monolayer membrane from **2** (green curve) on 330-nm-diameter SiO_2 spheres. Peak heights were normalized to the 315-nm emission of the SAM from **2**. (*F*) Raman spectra of a SAM (blue), linked monolayer (red), and transferred monolayer membranes on a Si wafer with 300 nm thermal SiO_2 (green) from **2**.

monolayer membrane from **2** transferred to a UV grade quartz slide reveals a small shift of the absorbance peak at 275 nm, but the absorption of poly(1,4-phenylene-1,3-butadiynylene) chromophores at 365 nm remains unchanged (Fig. 2*D*, green curve). When the monolayer membrane from **2** grown on silicon oxide beads were etched with aqueous HF, the fluorescence spectra (Fig. 2*E*, green curve) showed a slight increase in intensity, but no change in the overall peak signature (λ^{ex} = 370 nm). Finally, when a sample of monolayer membrane from **2** was transferred to a Si wafer with 300 nm thermal SiO_2, no change in the Raman peak at 2,204 cm^{-1}, corresponding to the C≡C stretching mode in diphenyl diacetylene, was observed (Fig. 2*F*, green curve). Together, these results suggest that the chemical nature of the monolayer membrane remains unchanged after HF etching and transfer.

We explored the modulus and structural integrity in two different types of experiments. First, the transfer of narrow ribbons of monolayer membranes to prestrained elastomeric substrates of poly(dimethylsiloxane) (PDMS) was studied. Releasing the prestrain leads to a nonlinear buckling instability that produces a one-dimensional, sinusoidal pattern of relief. Fig. 3*A* shows AFM images of a ribbon of a monolayer membrane from **2** before and after releasing the prestrain. This type of buckling response will only occur in ribbons of material with high levels of structural integrity and moduli that are much higher than the PDMS (29). Quantitative analysis of the buckling wavelength, with the known modulus of the PDMS (30) and the measured thickness of the monolayer membrane, yielded moduli between 1 and 10 GPa. These values are typical of polymers of similar materials. They are lower than single crystals of dicarbazolyl polydiacetylene (45 GPa) (31) and of graphene (≈1 TPa) (32). Second, to examine the structural integrity and barrier properties of SAMs, linked monolayers, and transferred monolayer membranes, we used wet etching based chemical amplification (33) to evaluate the area density of defects in the films. The defect densities in linked monolayers on their growth substrates [Si (100) with a native oxide layer] are 1.6×10^3, 1.4×10^3, and 9.1×10^2 defects per mm^2 for **1**, **2**, and **3**, respectively (Fig. 3*B Inset*). Several factors could contribute to the density of defects in the linked monolayers, such as defects on growth surfaces, defects in SAMs formation, and defects as a result of polymer shrinkage. Although polymer shrinkage may be an issue, especially for molecule **3**, it is challenging to assess its influence without information on packing density during the SAM formation. In particular, if the initial SAMs are packed very tightly, cross-linkage may actually result in expansion instead of shrinkage. The densities in linked monolayers are ≈10 times lower than those of the corresponding SAMs, suggesting a linking mechanism that tends to eliminate defects. The defect densities in the linked monolayers are, in fact, only slightly higher than well developed alkanethiolate SAMs on gold (33), which are known to have much better order and quality than SAMs of silanes. Similar studies performed on a monolayer membrane from **2** transferred to a substrate of Au(200 nm)/Cr(5 nm)/SiO_2(300 nm)/Si indicated a ≈10-fold increase in defect density compared with the same linked monolayer on its growth substrate (Fig. 3*A*). This increase is due, at least in part, to slight mechanical damage during transfer. Release of stresses associated with polymerization shrinkage could also contribute.

Although monolayer films are invisible on most substrates, we found that these transferred monolayer membranes could be visualized directly under an optical microscope when supported by oxidized Si substrates with an oxide layer of 300 nm, similar to observations in single-layer graphene (8). The Si wafer with 300 nm thermal SiO_2 was selected because the phase contrast between the monolayer membrane and the wafer results in a shift from violet-blue to blue (34). For all transferred films, we observed flat, continuous films largely free of defects over areas of several square millimeters (Fig. 3*C*). Near their edges, these monolayer membranes exhibited folds, holes, and tears, which we attribute to the transfer process.

The transferred monolayer membranes were also analyzed by AFM and transmission electron microscopy (TEM). A folded region of a transferred film from **1** showed clear correlations

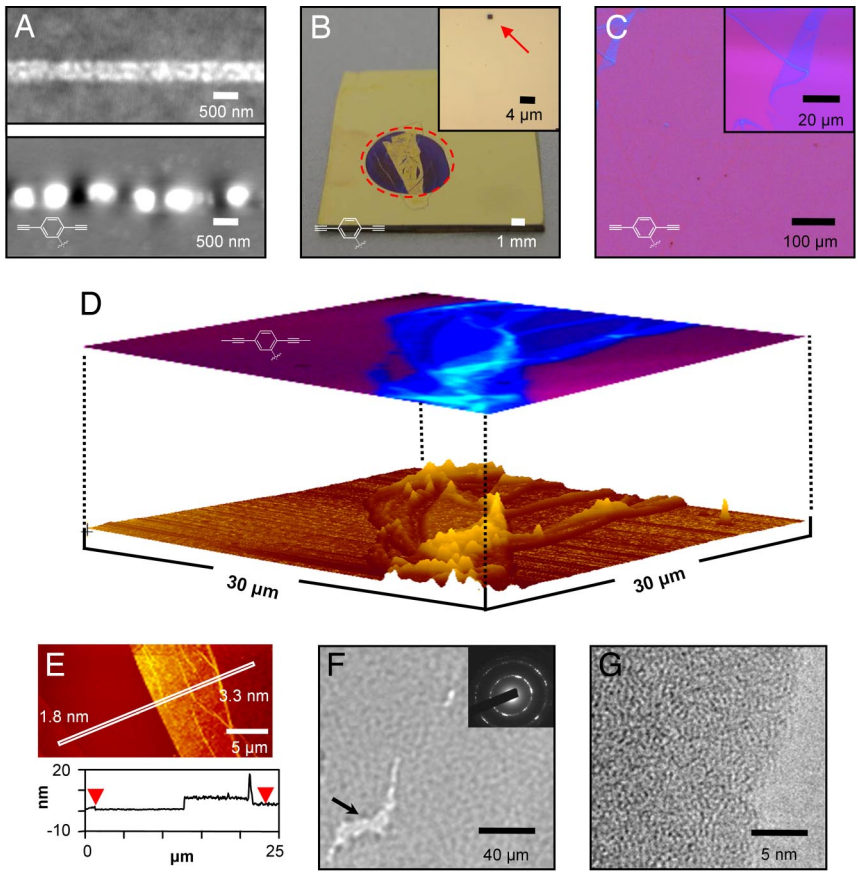

Fig. 3. Characterization of transferred monolayer membranes. (*A*) AFM images of a ribbon of a monolayer membrane from **2** (width = 500 nm) on a prestrained PDMS substrate before *(Upper)* and after (*Lower*) releasing the prestrain. (*B*) Image of a sample of monolayer membrane from **2** transferred to a substrate of Au(200 nm)/Cr(5 nm)/SiO_2(300 nm)/Si after wet etching the Au with a ferricyanide solution in a circular region (dashed line) surrounding the membrane. The etched areas appear as dark blue; the unetched gold region in the center corresponds to the transferred monolayer membranes. (*Inset*) An optical micrograph of a silicon substrate that supports a linked monolayer, collected after exposure to KOH etchant. The arrow indicates an etched pit corresponding to a pinhole defect in the monolayer. (*C*) Reflection mode optical micrograph of a monolayer membrane from **2** transferred to a Si wafer with a 300-nm thermal SiO_2 layer. (*Inset*) High-magnification micrograph of folds in the film. (*D*) Reflectance optical micrograph superimposed on tapping-mode AFM image of a monolayer membrane from **1** transferred to a Si wafer with a 300-nm thermal SiO_2 layer. (*E*) Tapping-mode AFM image and line-cut height profile showing a monolayer membrane from **1** with regions of 1.8- and 3.3-nm height, consistent with folding on transfer to a Si wafer with a 300-nm thermal SiO_2 layer. (*F*) Low-magnification TEM image of a monolayer membrane from **1** transferred to a holey carbon-coated grid. The arrow points toward a small defect in the film created by the transfer process. (*Inset*) An electron diffraction pattern with rings at 1.1 Å and 2 Å, but otherwise no significant in-plane ordering. (*G*) High-magnification TEM image of a monolayer membrane from 1 transferred to holey carbon-coated grid showing a film largely free of pinhole defects.

between thickness determined by tapping-mode AFM and intensity of the optical micrograph (Fig. 3*D*). The transferred monolayer membrane from **1** has a slightly increased thickness (1.8 nm) that likely results from a layer of water between the film and SiO_2 surface (8). Additionally, a folded area has a thickness (3.3 nm) that is approximately twice the nominal thickness for the rest of the film (Fig. 3*E*). The folding ability of these nanometer-thick films is a testament of their mechanical strength. TEM images of a monolayer membrane from **1** transferred to a holey carbon grid revealed a tightly packed monolayer with uniform thickness and very few pinhole defects that may have been invisible using AFM (Fig. 3 *F* and *G*).

The low density of defects and the high structural integrity of the linked monolayers allowed the creation of more exotic film geometries. Transfer of a monolayer membrane from **1** onto a substrate with an array of cylindrical holes (≈440 nm diameter, ≈400 nm depth) produces suspended monolayer "drumheads" that were nondestructively imaged by AFM and scanning electronic microscopy (SEM; Fig. 4 *A* and *B*). Again, the absence of torn regions illustrates the remarkable mechanical robustness of these systems.

The ability to form linked monolayers on a wide range of planar, nonplanar, or three-dimensional substrates creates further opportunities for fabrication of unusual structures. For example, a linked monolayer from **1** was formed directly on a substrate with an array of shallow voids (≈35 nm), to produce a continuous linked monolayer in the form of a 2D "pleated sheet" (Fig. 4 *C* and *D*). On transfer of the membrane, the AFM power spectrum shows an in-plane periodicity of the "pleats" that matches that of the growth substrate. However, the relief is only ≈1.2 nm, as might be expected from partial or complete folding of the monolayer membrane in the regions corresponding to the edges of relief in the substrate.

This strategy also allowed the formation of linked monolayers on 3D objects as well. SAMs of **1** were deposited on 226 ± 16 nm nonporous SiO_2 spheres with a procedure similar to that used for flat substrates. After linking, the SiO_2 substrate was removed by HF vapor etching to yield empty monolayer membrane "balloons." Fig. 4 shows TEM images of monolayer-coated spheres (Fig. 4*E*) and balloons (Fig. 4*F*). Histograms created from observation of many such objects show a close correspondence between sphere and balloon diameters, but the balloons

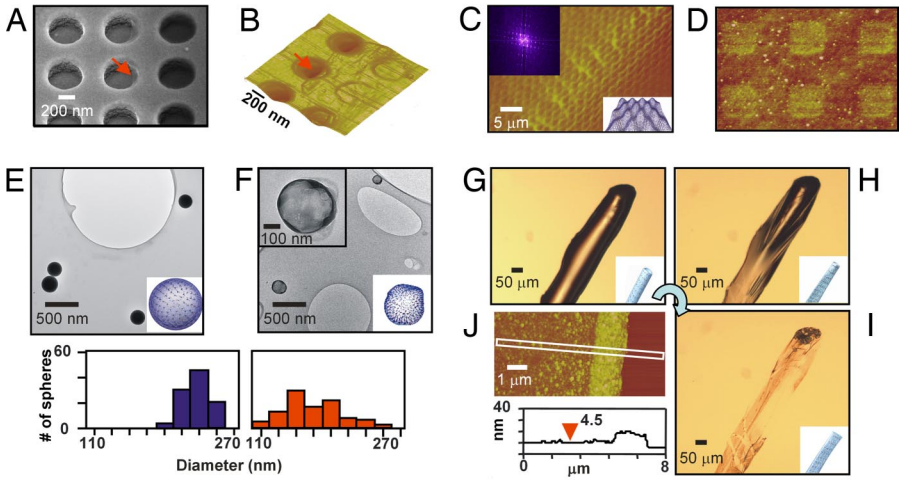

Fig. 4. Images of ''unusual'' monolayer membrane structures. (*A* and *B*) SEM and AFM images, respectively, of a membrane from **1** transferred onto a substrate with a square array of cylindrical holes (diameters ≈440 nm and depths ≈400 nm) to form ''drumhead'' structures. Red arrows point to the same region of the film that is suspended over the edge of a hole. (*C* and *D*) AFM and high-resolution AFM images, respectively, of a monolayer membrane from **1** grown on a substrate similar to that in *A*, but with relief depths of ≈35 nm, and then transferred to a flat Si wafer with a 300-nm thermal SiO_2 layer. (*C Inset Upper Left*) Power spectrum of the AFM image, indicating a well defined periodicity consistent with that of the growth substrate. (*C Inset Lower Right*) Illustration of a ''pleated sheet.'' (*E* and *F*) TEM images and diameter distributions of a monolayer membrane from **1** deposited on SiO_2 spheres imaged on a holey carbon-coated grid before (*E*) and after (*F*) HF vapor etching of the SiO_2. *Insets* are illustrations of the imaged structures. (*G–I*) Time-resolved reflection mode optical micrographs of a tubular membrane from **3** filled with HF/water immediately after HF vapor etching of optical fiber, after 20 min open to the air, and after complete drying, respectively. *Insets* are illustrations of the imaged structures. (*J*) AFM image of this collapsed tube. The line scan corresponds to an average over the area indicated by the rectangle.

have a slightly wider distribution and smaller size (diameters, 168 ± 32 nm) because of partial collapse on removal of the silica support. A similar process was carried out with ≈125-μm-diameter optical fibers by using SAMs of **3**. Immediately after the HF vapor etch, water droplets were observed within the hollow fibers. Fig. 4 *G*, *H*, and *I* show time-sequential optical micrographs illustrating evaporation of this encapsulated water. The AFM image in Fig. 4*J* shows that the monolayer membrane that remains after drying is consistent with the nominal layer thickness (≈4.5 nm center thickness), although capillary forces induced by the contracting HF/water droplet may be responsible for large nonuniformities near the edges. In a saturated environment, the water-filled monolayer membrane tubes maintain their shape for hours without tearing, providing additional evidence of their robustness.

A remaining topic of interest involves how the monolayer membranes are being held together. Although it could be envisioned that these membranes are being held together by polysiloxane formation during SAM deposition, transfer of *unlinked* SAMs of **1** and **2** yielded neither films nor film fragments. For the SAM of **3**, film fragments were observed but they were smaller and contained many more defects than the corresponding monolayer membrane. The small fragments in this case likely result from inadvertent cross-linking by air oxidation or by thermal polymerization under the SAM deposition conditions. Additionally, if these membranes were being held together through polysiloxanes it is highly unlikely that they would stand up to treatment with HF. Exposure of SAMs from **1** and **2** to the linkage conditions, yields linear oligomeric/polymer chains. Conceivably, these chains can be held together in a woven network, although this type of geometry is not necessary to explain the structural integrity of the films; previous studies of related systems indicate that purely noncovalent interactions can yield similar properties (13, 35). However, monolayer membranes from **3** are most likely held together because of multiple cross-linking. Both of these proposed mechanisms would explain the mechanical strength of the monolayer membranes on removal of the support and their flexibility to adopt the geometry of the given support.

Discussion

In conclusion, we have shown that linked carbon monolayers can be formed on a variety of solid surfaces. These linked monolayers are synthesized by linking three different alkyne-containing monomers with two different carbon–carbon bond-forming reactions [Mo(IV)-catalyzed alkyne metathesis and Cu-catalyzed Hay coupling]. The linked monolayers synthesized on flat surfaces have extremely large aspect ratios and are easily transferred from the native surface by protecting with photoresist and etching the inorganic substrate. These monolayer membranes are sufficiently robust to be suspended over 440-nm-diameter holes without tearing. The linked monolayers were also prepared on structured surfaces and 3D supports, and the freestanding monolayer membranes maintained the shape of the original support after etching. This approach to the synthesis of monolayer carbon networks provides a powerful method to explore the properties and device applications of a wide variety of carbon films. Other linking chemistries and monomers are currently being explored for the synthesis of conducting, 2D monolayer films.

Materials and Methods

Representative Synthesis of SAMs on Flat Substrates. A freshly cleaned and dried substrate was placed in a reaction vial containing a 0.015 M solution of **1** in toluene and TEA (10 mM) under a nitrogen atmosphere. The vial was sealed and heated to 95–100°C for 24 h. The substrate was removed and rinsed once with toluene, twice with dichloromethane, and sonicated for 5 min in toluene. The rinse was repeated and the substrate was sonicated for 5 min in methanol. The rinse was repeated and the substrate blown dry under a stream of nitrogen.

Synthesis of Linked Monolayers by Alkyne Metathesis. In a glovebox, 5.0 mg of trisamidomolybdenum(IV) propylidyne and 3.3 mg of *p*-nitrophenol were dissolved in 3 ml of trichlorobenzene in a reaction vial. The substrate was added, and the flask was sealed and placed under a vacuum (5 torr) for 22 h. The substrate was removed from the vial and rinsed once with dimethylfor-

mamide (DMF), once with a 0.1 M solution of sodium diethylcarbamodithioate in DMF, once with toluene, twice with dichloromethane, then sonicated in toluene for 5 min. The rinse was repeated and the substrate was sonicated for 5 min in methanol. The rinse was repeated a third time and the substrate was blown dry with a stream of nitrogen.

Synthesis of Linked Monolayers by Copper Coupling. In a reaction vial, 20 mg of CuCl was dissolved in 3 ml of degassed acetone. To this suspension was added 61 μl of TMEDA and the solution was allowed to stir under a nitrogen atmosphere at room temperature for 30 min. At this time, the substrates were added and the reaction vial purged with oxygen from a balloon. The mixture was stirred under an oxygen atmosphere for 15 h. The substrate was removed from the vial and rinsed once with DMF, once with a 0.1 M solution of sodium diethylcarbamodithioate in DMF, once with toluene, twice with dichloromethane, then sonicated in toluene for 5 min. The rinse was repeated and the substrate was sonicated for 5 min in methanol. The rinse was repeated a third time and the substrate was blown dry with a stream of nitrogen.

ACKNOWLEDGMENTS. We thank Prof. J. Notestein, Dr. T. Spila, Dr. R. Haasch, V. Petrova, Tu Truong, Prof. M. Shim, T. Banks, and K. Colravy for helpful discussions and help with analytical facilities. This work was supported by U.S. Department of Energy, Division of Materials Sciences Award DE-FG02-07ER46471, through the Frederick Seitz Materials Research Laboratory. All imaging and surface analysis, supported by Award DE-FG02-91ER45439, was performed at the Frederick Seitz Materials Research Laboratory Center for Microanalysis. S.U. was supported, in part, by the Anandamahidol Foundation.

1. Kroto HW, Heath JR, O'Brien SC, Curl RF, Smalley RE (1985) C_{60}: Buckminsterfullerene. *Nature* 318:162–163.
2. Krätschmer W, Lamb LD, Fostiropoulos K, Huffman DR (1990) Solid C_{60}: A new form of carbon. *Nature* 347:354–358.
3. Lu X, Chen Z (2005) Curved pi-conjugation, aromaticity, and the related chemistry of small fullerenes (C_{60}) and single-walled carbon nanotubes. *Chem Rev* 105:3643–3696.
4. Geim AK, Novoselov KS (2007) The rise of graphene. *Nat Mater* 6:183–191 and references therein.
5. Spitler EL, Johnson CA, II, Haley MM (2006) Renaissance of annulene chemistry. *Chem Rev* 106:5344–5386.
6. Tahara K, Yoshimura T, Sonoda M, Tobe Y, Williams RV (2007) Theoretical studies on graphyne substructures: Geometry, aromaticity, and electronic properties of the multiply fused dehydrobenzo[12]annulenes. *J Org Chem* 72:1437–1442.
7. Diederich F, Rubin Y (1992) Synthetic approaches toward molecular and polymeric carbon allotropes. *Angew Chem Int Ed* 31:1101–1123.
8. Novoselov KS, *et al.* (2004) Electric field effect in atomically thin carbon films. *Science* 306:666–669.
9. Berger C, *et al.* (2006) Electronic confinement and coherence in patterned epitaxial graphene. *Science* 312:1191–1196.
10. Wu J, Pisula W, Müllen K (2007) Graphenes as potential material for electronics. *Chem Rev* 107:718–747.
11. Chechik V, Crooks RM, Stirling CJM (2000) Reactions and reactivity in self-assembled monolayers. *Adv Mater* 12:1161–1171.
12. Eck W, Küller A, Grunze M, Völkel B, Gölzhäuser A (2005) Freestanding nanosheets from cross-linked biphenyl self-assembled monolayers. *Adv Mater* 17:2583–2587.
13. Arias-Marin E, *et al.* (2003) Amphiphilic phenyl-ethynylene polymers and copolymers. Synthesis, characterization, and optical emission properties. *Macromolecules* 36:3570–3579.
14. Decher G (2003) Polyelectrolyte multilayers, an overview. *Multilayer Thin Films*, eds Decher G, Schlenoff JB (Wiley-VCH, Weinheim, Germany), pp 1–46.
15. Rubner MF (2003) pH-Controlled fabrication of polyelectrolyte multilayers: Assembly and applications. *Multilayer Thin Films*, eds Decher G, Schlenoff JB (Wiley-VCH, Weinheim, Germany), pp 133–154.
16. Jiang C, Tsukruk VV (2006) Freestanding nanostructures via layer-by-layer assembly. *Adv Mater* 18:829–840.
17. Zhang W, Moore JS (2007) Alkyne metathesis: Catalysts and synthetic applications. *Adv Synth Catal* 349:93–120.
18. Siemsen P, Livingston RC, Diederich F (2000) Acetylenic coupling: A powerful tool in molecular construction. *Angew Chem Int Ed* 39:2633–2657.
19. Kim I-B, Dunkhorst A, Gilbert J, Bunz UHF (2005) Sensing of lead ions by a carboxylate-substituted PPE: Multivalency effects. *Macromolecules* 38:4560–4562.
20. Pelter A, Jones DE (2000) The preparation and some properties of substituted phenylene-ethynylene and phenylenebuta-1,3-diynylene polymers. *J Chem Soc, Perkin Trans 1* 14:2289–2294.
21. Anand S, *et al.* (2006) Optical excitations in carbon architectures based on dodecadehydrotribenzo[18]annulene. *J Phys Chem A* 110:1305–1318.
22. Patterson ML, Weaver MJ (1985) Surface-enhanced Raman spectroscopy as a probe of adsorbate-surface bonding: simple alkenes and alkynes adsorbed at gold electrodes. *J Phys Chem* 89:5046–5051.
23. Abramczyk H, Waliszewska G, Kolodziejski M (1998) Raman spectra of phenylacetylene in acetonitrile and methylcyclohexane at low temperatures. 2. Structural order and vibrational relaxation in frozen matrices at 77 K. *J Phys Chem A* 102:7765–7771.
24. Schrader B, *et al.* (2005) Non-destructive Raman analyses—Polyacetylenes in plants. *Spectrochim Acta Part A* 61:1395–1401.
25. Meskers SCJ, Peeters E, Langeveld-Voss BMW, Janssen RAJ (2000) Circular polarization of the fluorescence from films of poly(p-phenylene vinylene) and polythiophene with chiral side chains. *Adv Mater* 12:589–594.
26. Hittinger E, Kokil A, Weder C (2004) Synthesis and characterization of cross-linked conjugate polymers milli-, micro-, and nanoparticles. *Angew Chem Int Ed* 43:1808–1811.
27. Kim J, Swager TM (2001) Control of conformational and interpolymer effects in conjugated polymers. *Nature* 411:1030–1033.
28. Yam CM, Tong SSY, Kakkar AK (1998) Simple acid-base hydrolytic chemistry approach to molecular self-assembly: thin films of long chain alcohols terminated with alkyl, phenyl, and acetylene groups on inorganic oxides surfaces. *Langmuir* 14:6941–6947.
29. Khang D-Y, Jiang H, Huang Y, Rogers JA (2006) A stretchable form of single-crystal silicon for high-performance electronics on rubber substrates. *Science* 311:208–212.
30. Wilder EA, Guo S, Lin-Gibson S, Fasolka MJ, Stafford CM (2006) Measuring the modulus of soft polymer networks via a buckling-based metrology. *Macromolecules* 39:4138–4143.
31. Galiotis C, *et al.* (1984) High-modulus polydiacetylene single-crystal fibers. *J Polym Sci Polym Phys Ed* 22:1589–1606.
32. Bunch JS, *et al.* (2007) Electromechanical resonators from graphene sheets. *Science* 315:490–493.
33. Zhao X-M, Wilbur JL, Whitesides GM (1996) Using two-stage chemical amplification to determine the density of defects in self-assembled monolayers of alkanethiolates on gold. *Langmuir* 12:3257–3264.
34. Henrie J, Kellis S, Schultz SM, Hawkins A (2004) Electronic color charts for dielectric films on silicon. *Opt Express* 12:1464–1469.
35. Day D, Lando JB (1980) Morphology of crystalline diacetylene monolayers polymerized at the gas-water interface. *Macromolecules* 13:1478–1483.

Supporting Information

Schultz *et al.* 10.1073/pnas.0710081105

STXT

SI Text

General. All reagents were purchased and used as received without further purification unless otherwise noted. THF was dried by distilling from a sodium benzophenone ketyl. Triethylamine was dried by distilling from CaH_2. Toluene, methanol, and dichloromethane were dried by passing through a column of activated alumina before use. Ethanol was dried by distilling from magnesium ethoxide. Silicon nitride was deposited by plasma-enhanced chemical vapor deposition (PECVD) onto a silicon wafer with a 300-nm thermal oxide (Process Specialties Inc.). TEM was performed on a JEOL 2010 LaB6 TEM. SEM was performed on a Hitachi S-4700 high-resolution SEM. AFM was performed on a Digital Instruments Dimension 3100 AFM.

Synthesis of Monomers:

2-(2,5-dibromobenzyloxy)-tetrahydro-2H-pyran.

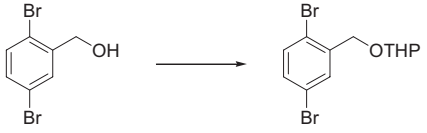

In a 250-ml flame-dried, round-bottom flask equipped with a stir bar was placed 2.13 g of 2,5-dibromobenzyl alcohol (8.00 mmol, 1.00 eq) and 0.041 g of TsOH-H_2O (0.24 mmol, 0.03 eq) in 40 ml of dichloromethane. To the suspension was added 2.0 ml of dihydropyran (24.0 mmol, 3.0 eq) by syringe. The reaction mixture was allowed to stir under a N_2 atmosphere at room temperature for 12 h. The reaction mixture was transferred to a separatory funnel, diluted with 50 ml of dichloromethane and washed twice with 20 ml of water and once with 20 ml of brine. The organic layer was dried over $MgSO_4$, filtered, and the solvent was removed *in vacuo*. The crude material was purified by column chromatography eluting with 10% dichloromethane/hexanes to 20% dichloromethane/hexanes to yield 2.26 g of a clear oil (90% yield).

2-(2,5-dibromobenzyloxy)-tetrahydro-2H-pyran. TLC (EtOAc:Hexanes, 1:4 vol/vol): R_f = 0.55; ^{1}H NMR (500 MHz, $CDCl_3$): δ 1.53–1.69 (m, 3H), 1.70–1.84 (m, 2H), 1.85–1.96 (m, 1H), 3.55–3.61 (m, 1H), 3.87–3.93 (m, 1H), 4.51 (d, J = 13.7 Hz, 1H), 4.77 (d, J = 13.7 Hz, 1H), 4.78 (d, J = 3.3 Hz, 1H), 7.27 (dd, J = 8.5 Hz, J = 2.5 Hz, 1H), 7.39 (d, J = 8.5 Hz, 1H), 7.66 (d, 2.5, 1H); ^{13}C NMR (75 MHz $CDCl_3$): δ 19.2, 25.3, 30.4, 62.1, 67.8, 98.4, 120.7, 121.4, 131.4, 131.5, 133.6, 140.0; IR: 3054, 2987, 2948, 1266, 734; E.I.-HRMS (*m*/*z*): $[M]^+$ calculated for $C_{12}H_{14}Br_2O_2$, 347.9361; found, 347.9363.

2-(2,5-Diethynylbenzyloxy)-tetrahydro-2H-pyran.

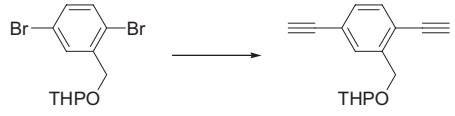

In a 50-ml sealed flask equipped with a stir bar under an argon atmosphere was dissolved 0.71 g of 2-(2,5-dibromobenzyloxy)-tetrahydro-2H-pyran (2.00 mmol, 1.00 eq), 0.60 g of trimethylsilyl acetylene (6.00 mmol, 3.00 eq), 0.057 g $Pd(PPh_3)_2Cl_2$ (0.081 mmol, 0.040 eq), 0.080 g PPh_3 (0.031 mmol, 0.15 eq), and 0.039 g CuI (0.20 mmol, 0.10 eq) in 12 ml of triethylamine and 8 ml of THF. The flask was sealed and heated to 80°C for 12 h. The mixture was allowed to cool to room temperature, filtered, and the solvent was removed *in vacuo*. The crude material was filtered through a plug of silica eluting with 1:1 DCM/Hexanes and the crude product was taken on to the next step without further purification.

The bis(TMS acetylene) was dissolved in 12 ml of a 1:1 mixture of MeOH and DCM in a 50-ml round-bottom flask equipped with a stir bar. To the mixture was added 0.66 g of K_2CO_3 (4.80 mmol, 2.40 eq). After stirring for 12 h under a nitrogen atmosphere at ambient temperature, the mixture was transferred to a separatory funnel and diluted with 30 ml of a saturated solution of NH_4Cl. The aqueous layer was extracted three times with 10 ml of ethyl acetate. The organic extracts were combined and washed once with 10 ml of brine. The organic layer was dried over $MgSO_4$, filtered, and the solvent was removed *in vacuo*. The crude material was purified by column chromatography eluting with 10% DCM/hexanes to 40% DCM/hexanes to yield 0.42 g of a light orange oil (87% yield over two steps).

2-(2,5-diethynylbenzyloxy)-tetrahydro-2H-pyran. TLC (DCM:Hexanes, 3:7 vol/vol): R_f = 0.25; ^{1}H NMR (400 MHz, $CDCl_3$): δ 1.51–1.67 (bm, 3H), 1.68–1.83 (bm, 2H), 1.84–1.96 (bm, 1H), 3.17 (s, 1H), 3.38 (s, 1H), 3.53–3.61 (m, 1H), 3.88–3.96 (m, 1H), 4.66 (d, J = 13.8 Hz, 1H), 4.78 (t, J = 3.4 Hz, 1H), 4.90 (d, J = 13.8 Hz, 1H), 7.66 (dd, J = 8.0 Hz, J = 1.5 Hz, 1H), 7.43 (d, J = 8.0 Hz, 1H), 7.65 (d, J = 1.5 Hz, 1H); ^{13}C NMR (75 MHz, $CDCl_3$): δ 19.5, 25.7, 30.7, 62.3, 66.9, 79.1, 80.9, 83.5, 83.8, 98.7, 121.0, 122.9, 130.9, 131.0, 132.7, 141.5; IR: 3289, 2944, 2871, 1201, 1129, 1034; E.I.-HRMS (*m*/*z*): $[M]^+$ calculated for $C_{16}H_{16}O_2$, 240.1150; found, 240.1154.

(2,5-Diethynylphenyl)methanol.

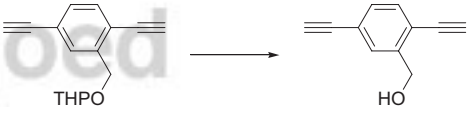

To a solution of 0.10 g of 2-(2,5-diethynylbenzyloxy)-tetrahydro-2H-pyran dissolved in 2.5 ml of MeOH in a 10-ml round-bottom flask was added 0.016 g of TsOH-H_2O (0.084 mmol, 0.20 eq). The flask was sealed under a nitrogen atmosphere and allowed to stir for 12 h at ambient temperature. The reaction mixture was transferred to a separatory funnel and diluted with 15 ml of H_2O and extracted three times with 5 ml of DCM. The organic extracts were combined, washed one time with 10 ml of brine, dried over $MgSO_4$, filtered, and the solvent was removed *in vacuo*. The crude material was purified by column chromatography eluting with 50% DCM/Hexanes to DCM to yield 46 mg of a tan solid (71% yield).

(2,5-diethynylphenyl)methanol. mp: 70.5–71.5°C; TLC (DCM:Hexanes, 2:3 vol/vol): R_f = 0.18; ^{1}H NMR (500, MHz $CDCl_3$): δ 1.16 (t, J = 6.1 Hz, 1H), 3.17 (s, 1H), 3.42 (s, 1H), 4.81 (d, J = 6.1 Hz, 2H), 7.37 (dd, J = 8.0 Hz, J = 1.5 Hz, 1H), 7.44 (d, J = 8.0 Hz, 1H), 7.59 (dd, J = 1.5 Hz, 1H); ^{13}C NMR (75 MHz, $CDCl_3$): δ 63.3, 79.1, 80.6, 83.0, 83.7, 120.5, 122.9, 130.7, 130.9, 132.7, 143.3; IR: 3275, 2925, 2867, 1048, 1026, 890, 828, 690, 623; E.I.-HRMS (*m*/*z*): $[M]^+$ calculated for $C_{11}H_8O$, 156.0575; found, 156.0573.

2,5-Diethynylbenzyl 3-(triethoxysilyl)propylcarbamate (2).

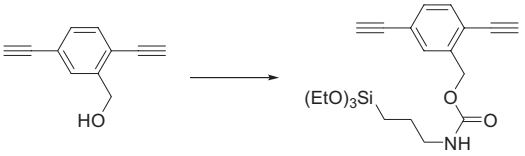

In an oven-dried, 10-ml Schlenk flask equipped with a stir bar, was dissolved 0.080 g of (2,5-diethynylphenyl)methanol (0.51 mmol, 1.0 eq) in 3 ml of THF under a N_2 atmosphere. To this solution was added 0.16 ml of triethoxy(3-isocyanatopropyl)si-

lane (0.67 mmol, 1.3 eq) and 3.0 μl of dibutyltin dilaurate (0.005 mmol, 0.01 eq) by syringe. The flask was sealed and heated to 60°C. After 18 h, the reaction mixture was cooled to ambient temperature and the solvent was removed *in vacuo*. The crude material was purified by column chromatography eluting with 7–20% EtOAc/hexanes to yield 0.17 g of a light-orange liquid (81% yield).

2,5-diethynylbenzyl 3-(triethoxysilyl)propylcarbamate. TLC (EtOAc:Hexanes, 1:4 vol/vol): R_f = 0.19; ^{1}H NMR (500 MHz $CDCl_3$): δ 0.59–0.66 (m, 2H), 1.2 (t, J = 7.0 Hz, 9H), 1.57–1.68 (m, 2H), 3.16 (s, 1H), 3.17–3.24 (m, 2H), 3.41 (s, 1H), 3.81 (q, J = 7.0 Hz, 6H), 5.12 (bs, 1H), 5.23 (s, 2H), 7.36 (dd, J = 8.0 Hz, J = 1.3 Hz, 1H), 7.43 (d, J = 8.0 Hz, 1H), 7.52 (d, J = 1.3 Hz, 1H); ^{13}C NMR (75 MHz $CDCl_3$): δ 7.6, 18.2, 23.2, 43.5, 58.4, 63.9, 79.1, 80.2, 82.9, 83.9, 121.3, 122.7, 131.2, 132.6, 156.1; IR: 3295, 2975, 2927, 2886, 1717, 1700, 1540, 1246, 1077, 957; E.I.-HRMS (*m/z*): $[M]^+$ calculated for $C_{21}H_{29}NO_5Si$, 403.1815; found, 403.1813.

2-(2,5-Di(prop-1-ynyl)benzyloxy)-tetrahydro-2H-pyran.

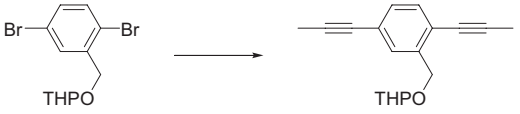

In a glove box, 0.11 g of prop-1-ynyllithium (2.40 mmol, 3.00 eq) and 0.50 g of zinc bromide (2.20 mmol, 2.80 eq) were dissolved in 3 ml of THF. This solution was then added to a solution of 0.28 g of 2-(2,5-dibromobenzyloxy)-tetrahydro-2H-pyran dissolved in 1.5 ml of THF in a Schlenk tube. To the mixture was added 0.091 g of $Pd(PPh_3)_4$ (0.079 mmol, 0.10 eq). The flask was sealed and heated to 60°C for 12 h. The reaction was allowed to cool to ambient temperature, transferred to a separatory funnel, and 25 ml of a saturated solution of NH_4Cl was added. The aqueous layer was extracted three times with 10 ml of diethyl ether. The combined organic layers were washed with 10 ml of brine, dried over $MgSO_4$, filtered, and the solvent was removed *in vacuo*. The crude product was purified by column chromatography, eluting with 5% diethyl ether/hexanes to yield 0.18 g of a white solid (86% yield).

2-(2,5-Di(prop-1-ynyl)benzyloxy)-tetrahydro-2H-pyran. mp: 56–58°C; TLC (EtOAc:Hexanes, 1:4 vol/vol): R_f = 0.4; ^{1}H NMR (500 MHz, $CDCl_3$): δ 1.49–1.68 (m, 3H), 1.69–1.82 (m, 2H), 1.86–1.96 (m, 1H), 2.05 (s, 3H), 2.08 (s, 3H), 3.53–3.59 (m, 1H), 3.90–3.97 (m, 1H), 4.60 (d, 13.2, 1H), 4.76–4.79 (m, 1H), 4.85 (d, J = 13.2 Hz, 1H), 7.21 (dd, J = 8.5 Hz, J = 1.8 Hz, 1H), 7.28 (d, J = 8.5 Hz, 1H), 7.50 (d, J = 1.8 Hz, 1H); ^{13}C NMR (75 MHz, $CDCl_3$): δ 4.4, 4.6, 19.2, 25.4, 30.5, 61.8, 66.9, 77.1, 79.7, 87.1, 91.8, 98.2, 121.4, 123.2, 129.92, 129.93, 131.8, 140.2; IR: 2943, 2868, 1486, 1201, 1130, 1033; C.I.-HRMS (*m/z*): $[M+H]^+$ calculated, 269.1542; found, 269.1548.

2,5-Di(prop-1-ynyl)benzyl 3-(triethoxysilyl)propylcarbamate (1).

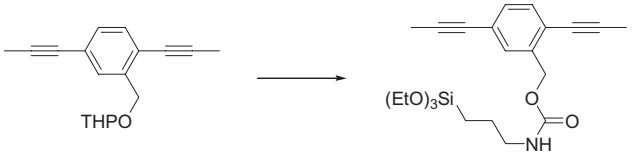

In a 25-ml flame-dried, round-bottom flask was dissolved 0.14 g of 2-(2,5-di(prop-1-ynyl)benzyloxy)-tetrahydro-2H-pyran (0.54 mmol, 1.00 eq) in 2.5 ml of MeOH and 1 ml of dichloromethane. To this solution was added 0.020 mg of TsOH-H_2O (0.11 mmol, 0.20 eq) and the reaction mixture was allowed to stir for 12 h under a N_2 atmosphere at room temperature. The reaction mixture was transferred to a separatory funnel and diluted with 25 ml of a saturated solution of $NaHCO_3$. The aqueous layer was extracted three times with 10 ml of dichloromethane. The combined extracts were washed once with 10 ml of brine, dried over $MgSO_4$, filtered, and the solvent was removed *in vacuo* to yield a white solid. The solid was dissolved in 3 ml of dry THF and placed under a N_2 atmosphere. To this solution was added 0.17 ml of triethoxy(3-isocyanatopropyl)silane (0.70 mmol, 1.30 eq) and 3.2 μl of dibutyltin dilaurate (0.0054 mmol, 0.010 eq) by syringe. A condenser was attached to the flask, and the reaction mixture was heated to reflux under a N_2 atmosphere. After 18 h, the reaction mixture was cooled to ambient temperature and the solvent was removed *in vacuo*. The crude material was purified by column chromatography eluting with 10% acetone/hexanes to yield 210 mg of a white solid (86% yield over two steps).

2,5-di(prop-1-ynyl)benzyl 3-(triethoxysilyl)propylcarbamate. mp: 54–56°C; TLC (EtOAc:Hexanes, 3:7 vol/vol) R_f = 0.4; ^{1}H NMR (500 MHz, CD_2Cl_2): δ 0.57 (m, 2H), 1.20 (t, J = 7.1 Hz, 9H), 1.54–1.66 (m, 2H), 2.04 (s, 3H), 2.08 (s, 3H), 3.13–3.21 (m, 2H), 3.80 (q, J = 7.1 Hz, 6H), 5.06–5.13 (bs, 1H), 5.16 (s, 2H), 7.22 (d, J = 8.0 Hz, 1H), 7.29 (d, J = 8.0 Hz, 1H), 7.37 (s, 1H); ^{13}C NMR (75 MHz, CD_2Cl_2): δ 4.4, 4.6, 7.9, 18.4, 23.7, 43.9, 50.6, 64.5, 76.9, 79.5, 87.8, 92.9, 122.3, 123.7 130.65, 130.74, 132.2, 139.0, 156.4; IR: 3328, 2974, 2927, 2884, 1696, 1540, 1282, 1259, 1082; C.I.-HRMS (*m/z*): $[M]^+$ calculated, 432.2206; found, 432.2205.

3,3-Diethyl-1-(2,4,5-tribromophenyl)triaz-1-ene.

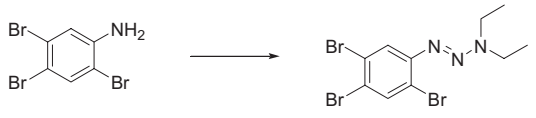

In a stirred solution of 0.93 g of 2,4,5-tribromoaniline (2.80 mmol, 1.00 eq) dissolved in 6 ml of acetonitrile, 2 ml of THF, and 3 ml of water in a 100-ml round-bottom flask, was added with 2.4 ml of concentrated HCl (28.3 mmol, 10.0 eq) to form a light-orange slurry. The mixture was cooled to −10°C and a solution of 0.41 g of $NaNO_2$ (5.90 mmol, 2.10 eq) dissolved in 2 ml of water and 1 ml of acetonitrile was added dropwise by syringe over 20 min maintaining a temperature below −5°C. The mixture was stirred for an additional 15 min at −10°C and then transferred by cannulation to a solution of 2.1 g of diethylamine (28.3 mmol, 10.0 eq) and 19.6 g of K_2CO_3 (14.2 mmol, 10.0 eq) dissolved in 6 ml of acetonitrile and 12 ml of water maintaining a temperature <0°C. This mixture was allowed to warm to room temperature and stirred for 4 h. The mixture was transferred to a separatory funnel, diluted with 100 ml of diethylethe,r and washed twice with 100 ml of brine. The organic layer was dried over $MgSO_4$, filtered, and the solvent was removed *in vacuo*. The crude material was purified by column chromatography eluting with 3% DCM/hexanes to yield 0.70 g of an orange solid (60% yield).

3,3-diethyl-1-(2,4,5-tribromophenyl)triaz-1-ene. mp: 46–50°C; TLC (DCM:Hexanes, 1:4 vol/vol): R_f = 0.42; ^{1}H NMR (500 MHz, $CDCl_3$): δ 1.2–1.5 (bd, 6H), 3.80 (bs, 4H), 7.66 (s, 1H), 7.80 (s, 1H); ^{13}C NMR (75 MHz, $CDCl_3$): δ 10.6, 14.4, 42.3, 49.5, 118.7, 119.8, 122.4, 123.8, 136.4, 148.4; IR: 3079, 2973, 2930, 2867, 1440, 1401, 1328, 1109, 1042, 884; E.I.-HRMS (*m/z*): $[M]^+$ calculated for $C_{10}H_{12}Br_3N_3$, 410.8581; found, 410.8585.

3,3-Diethyl-1-(2,4,5-Tris((trimethylsilyl)ethynyl)phenyl)triaz-1-ene.

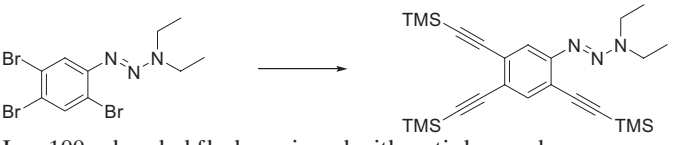

In a 100-ml sealed flask equipped with a stir bar under an argon atmosphere was dissolved 1.7 g of 3,3-diethyl-1-(2,4,5-tribromophenyl)triaz-1-ene (4.0 mmol, 1.0 eq), 1.8 g of trimethylsilyl acetylene (18.0 mmol, 4.5 eq), 0.14 g of $Pd(PPh_3)_2Cl_2$ (0.20 mmol, 0.050 eq), 0.21 g of PPh_3 (0.80 mmol, 0.20 eq), and 76.0 mg of CuI (0.4 mmol, 0.1 eq) in 40 ml of a 1:1 mixture of TEA/THF. The flask was sealed and heated to 70°C for 12 h. The mixture was allowed to cool to room temperature, filtered, and the solvent was removed *in vacuo*. The crude material was

purified by column chromatography eluting with 5% Et_2O/hexanes to yield 1.7 g of a light-yellow solid (94% yield).

(3,3-diethyl-1-(2,4,5-Tris((trimethylsilyl)ethynyl)phenyl)triaz-1-ene. mp: 104–108°C; TLC (EtOAc:Hexanes, 1:4 vol/vol): R_f = 0.68; ^{1}H NMR (400 MHz, $CDCl_3$): δ 0.22 (s, 9H), 0.25 (s, 9H), 0.26 (s, 9H), 1.22–1.38 (bm, 6H), 3.72–3.86 (bs, 4H), 7.51 (s, 1H), 7.60 (s, 1H); ^{13}C NMR (75 MHz, $CDCl_3$): δ −0.04, 0, 0.1, 11.0, 14.5, 42.0 49.4, 97.9, 99.1, 100.1, 102.1, 102.9, 103.4, 118.2, 120.2, 121.5, 125.9, 137.3, 151.8; IR: 2960, 2152, 1379, 1249, 841; E.I.-HRMS (*m*/*z*): $[M]^+$ calculated for $C_{25}H_{39}N_3Si_3$, 465.2452; found, 465.2447.

(5-Iodobenzene-1,2,4-triyl)Tris(ethyne-2,1-diyl)Tris(trimethylsilane).

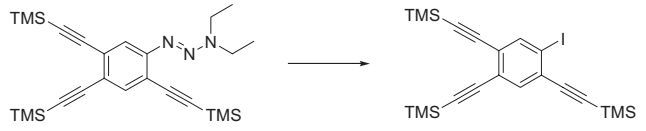

A solution of 0.28 g of (3,3-diethyl-1-(2,4,5-Tris((trimethylsilyl-)ethynyl)phenyl)triaz-1-ene (0.59 mmol) dissolved in 5.9 ml of iodomethane was placed in a sealed flask under a nitrogen atmosphere and heated to 125°C for 14 h. The mixture was allowed to cool to room temperature and a small amount of silica was added. The solvent was removed *in vacuo* and the crude material was purified by column chromatography eluting with 2% DCM/hexanes to yield 0.26 g of a yellow solid (88% yield).

(5-iodobenzene-1,2,4-triyl)Tris(ethyne-2,1-diyl)Tris(trimethylsilane). mp = 85–88°C; TLC (EtOAc:Hexanes, 1:4 vol/vol): R_f = 0.76; ^{1}H NMR (400 MHz, $CDCl_3$): δ 0.22 (s, 9H), 0.25 (s, 9H), 0.26 (s, 9H), 7.54 (s, 1H), 7.92 (s, 1H); ^{13}C NMR (75 MHz, $CDCl_3$): δ −0.34, −0.14, 98.9, 100.4, 101.2, 101.3, 101.5, 101.7, 125.5, 126.5, 129.5, 135.6, 141.9; IR: 2957, 2897, 2159, 1462, 1248, 841, 761; E.I.-HRMS (*m*/*z*): $[M]^+$ calculated for $C_{21}H_{29}ISi_3$, 492.0622; found, 492.0671.

(2,5-Bis((2,4,5-Tris((trimethylsilyl)ethynyl)phenyl)ethynyl)phenyl) methanol.

In a 20-ml sealed flask equipped with a stir bar under an argon atmosphere was dissolved 0.11 g of 2-(2,5-diethynylbenzyloxy)-tetrahydro-2H-pyran (0.45 mmol, 1.00 eq), 0.49 g of (5-iodobenzene-1,2,4-triyl)Tris(ethyne-2,1-diyl)Tris(trimethylsilane) (1.00 mmol, 2.20 eq), 0.016 g of $Pd(PPh_3)_2Cl_2$ (0.023 mmol, 0.050 eq), 0.012 g of PPh_3 (0.045 mmol, 0.10 eq), and 8.6 mg of CuI (0.05 mmol, 0.1 eq) in 3 ml of triethylamine and 2 ml of THF. The flask was sealed and stirred at room temperature for 8 h, then heated to 45°C for 12 h. The mixture was allowed to cool to room temperature, filtered, and the solvent was removed *in vacuo*. The crude material was purified by column chromatography eluting with 10% EtOAc/hexanes then 7% acetone/hexanes to produce a light-yellow solid that was not be purified further.

To the crude solid was added 6 ml of MeOH and ≈2 ml of DCM followed by 17.0 mg of TsOH-H_2O (0.09 mmol, 0.2 eq). The mixture was allowed to stir overnight at room temperature under a N_2 atmosphere. The reaction mixture was transferred to a separatory funnel, diluted with 30 ml of a saturated solution of $NaHCO_3$, and extracted three times with 15 ml of DCM. The organic extracts were combined and washed one time with 10 ml of brine, dried over $MgSO_4$, filtered, and the solvent was removed *in vacuo*. The crude product was purified by column chromatography eluting with 4% acetone/hexanes to 15% acetone/hexanes to yield 0.27 g of a light-yellow solid (68% yield over two steps). All chromatography solvents contained ≈0.5% triethylamine.

(2,5-bis((2,4,5-Tris((trimethylsilyl)ethynyl)phenyl)ethynyl)phenyl)methanol. mp: dec. 135°C; TLC (DCM:Hexanes, 1:4 vol/vol): R_f = 0.36; ^{1}H NMR (500 MHz, $CDCl_3$): δ 0.26–0.32 (m, 54H), 4.89 (s, 2H), 7.44 (dd, J = 7.9 Hz, J = 1.7 Hz, 1H), 7.52 (d, J = 7.9 Hz, 1H), 7.59–7.66 (m, 5H); ^{13}C NMR (75 MHz, $CDCl_3$): δ −0.1, 0, 63.6, 89.5, 92.7, 94.0, 95.4, 101.5, 101.6, 101.7, 101.75, 101.8, 101.9, 102.1, 102.15, 102.2, 102.25, 102.3, 102.5, 125.1, 125.4, 125.6, 125.7, 125.8, 125.9, 126.0, 130.5, 130.9, 132.8, 135.8, 135.9, 136.4, 136.9, 143.9; IR: 2959, 2899, 2157, 1250, 879, 842, 760; E.I.-MS (*m*/*z*): $[M]^+$ calculated for $C_{53}H_{64}OSi_6$, 884.3573; found, 884.3577.

2,5-Bis((2,4,5-triethynylphenyl)ethynyl)benzyl 3-(triethoxysilyl) propylcarbamate (3).

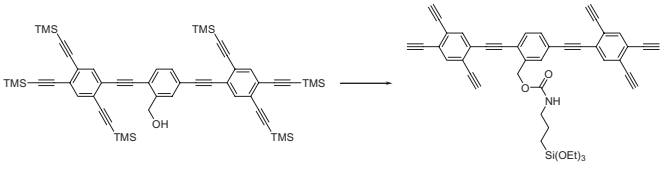

To a solution of 0.24 g of (2,5-bis((2,4,5-Tris((trimethylsilyl)ethynyl)phenyl)ethynyl) phenyl)methanol (0.27 mmol, 1.00 eq) dissolved in 3 ml of MeOH and 3 ml of THF was added 0.33 g of K_2CO_3 (2.44 mmol, 9.00 eq). After stirring for 8 h at room temperature, the slurry was transferred to a separatory funnel, diluted with 25 ml of brine, and extracted three times with 15 ml of THF. The organic extracts were combined and washed with 10 ml of brine, dried over $MgSO_4$, filtered through a plug of silica, and the solvent was removed *in vacuo*.

The crude solid was dissolved in 5 ml of THF in a 25-ml Schlenk flask under a nitrogen atmosphere. To the flask was added 0.087 ml of triethoxy(3-isocyanatopropyl)silane (0.35 mmol, 1.30 eq) and 1.6 μl of dibutyltin dilaurate (0.002 mmol, 0.01 eq). The flask was sealed and heated to 55°C for 18 h. The solvent was removed *in vacuo* and the crude material was purified by column chromatography eluting with 40% DCM/hexanes then 40% DCM/10% acetone/hexanes all containing ≈0.5% TEA to yield 116 mg of a light-yellow solid (60% yield over two steps).

2,5-bis((2,4,5-triethynylphenyl)ethynyl)benzyl 3-(triethoxysilyl)propylcarbamate. mp: dec. 125°C; TLC (Acetone:Hexanes, 1:1 vol/vol) R_f = 0.65; ^{1}H NMR (500 MHz, $CDCl_3$): δ 0.55–0.71 (m, 2H), 1.21 (t, J = 6.9, 9H) 1.60–1.70 (m, 2H), 3.19–3.27 (m 2H), 3.42–3.46 (m, 4H), 3.50 (s, 1H), 3.72, (s, 1H), 3.81 (q, J = 6.9 Hz, 6H), 5.12–5.19 (bs, 1H), 5.39, (s, 2H), 7.47 (d, J = 8.1 Hz, 1H), 7.50 (d, J = 8.1 Hz, 1H), 7.63 (s, 1H), 7.65–7.70 (m, 4H); ^{13}C NMR (75 MHz, CD_2Cl_2): δ 7.9, 18.5, 23.6, 43.9, 58.7, 64.7, 80.75, 80.80, 80.85, 80.9, 81.0, 83.69, 83.71, 83.75, 83.8, 84.0, 85.1, 89.0, 92.9, 93.7, 95.6, 121.9, 123.7, 125.13, 125.15, 125.2, 125.22, 125.5, 125.6, 126.4, 126.5, 130.9, 131.2, 132.9, 136.1, 136.2, 136.8, 136.9, 140.0, 156.4; IR: 3286, 2973, 2926, 2884, 1685, 1498, 1252, 1078; FAB-HRMS (*m*/*z*): $[M]^+$ calculated for $C_{45}H_{37}NO_5Si$, 699.2441; found, 699.2442.

Preparation of Flat Samples. Silicon oxide, silicon nitride, and quartz (75 mm × 25 mm × 1 mm purchased from Chemglass) substrates were cleaned before use by heating to 90°C in a 3:1 H_2SO_4/H_2O_2 solution for 2 h (caution**:** piranha solution is explosive and care should be taken while using this mixture). The substrates were rinsed thoroughly with deionized water, then blown dry with a stream of nitrogen.

Representative Synthesis of SAMs on Flat Substrates. A freshly cleaned and dried substrate was placed in a reaction vial containing a 0.015 M solution of 2,5-di(prop-1-ynyl)benzyl 3-(triethoxysilyl)propylcarbamate in toluene and TEA (10 mM) under a nitrogen atmosphere. The vial was sealed and heated to

95–100°C for 24 h. The substrate was removed and rinsed once with toluene, twice with dichloromethane, and sonicated for 5 min in toluene. The rinse was repeated and the substrate was sonicated for 5 min in methanol. The rinse was repeated and the substrate blown dry under a stream of nitrogen.

Preparation of SiO_2 and Spheres and Glass Fibers. Nonporous 330-nm SiO_2 spheres purchased from Bangs Laboratories and 125-μm optical fibers (stripped of acrylate coating) purchased from Thorlabs were cleaned by heating to 90°C for 2 h in a 6 M solution of HCl. The objects were rinsed with water, methanol, and dichloromethane followed by drying under vacuum at 100°C overnight.

Representative Synthesis of SAMs on Objects. Freshly cleaned and dried objects were placed in a reaction vial containing a 0.015 M solution of 2,5-di(prop-1-ynyl)benzyl 3-(triethoxysilyl)propylcarbamate in ethanol and TEA (10 mM) under a nitrogen atmosphere. The vial was sealed, heated to 95–100°C, and stirred by a rotatory plate for 24 h. The substrates were removed and rinsed twice with methanol, twice with dichloromethane, and sonicated for 5 min in methanol.

Synthesis of C^3Ms on Flat Surfaces by Mo(IV) Alkyne Metathesis. In a glovebox, 5.0 mg of trisamidomolybdenum(IV) propylidyne (*1*) and 3.3 mg of *p*-nitrophenol were dissolved in 3 ml of trichlorobenzene in a reaction vial. The substrate was added, the flask was sealed, and then place under a vacuum of ≈20 in of Hg for 22 h. The substrate was removed from the vial and rinsed once with DMF, once with a 0.1 M solution of sodium diethylcarbamodithioate in DMF, once with toluene, twice with dichloromethane, then sonicated in toluene for 5 min. The rinse was repeated and the substrate was sonicated for 5 min in methanol. The rinse was repeated a third time and the substrate was blown dry with a stream of nitrogen.

Synthesis of C^3Ms on Objects by Mo(IV) Alkyne Metathesis. The same procedure used for flat surfaces was followed, except objects were cleaned by transferring to microcentrifuge tubes exposed to repeated washing/centrifuge cycles with same solvents as above.

Synthesis of C^3Ms by Cu-coupling. In a reaction vial was dissolved 20 mg of CuCl in 3 ml of dry, degassed acetone. To this suspension was added 61 μl of TMEDA and the solution was allowed to stir under a nitrogen atmosphere at room temperature for 30 min. At this time, the substrates were added and the reaction vial purged with oxygen from a balloon. The mixture was stirred under an oxygen atmosphere for 15 h. The substrate was removed from the vial and rinsed once with DMF, once with a 0.1 M solution of sodium diethylcarbamodithioate in DMF, once with toluene, twice with dichloromethane then sonicated in toluene for 5 min. The rinse was repeated and the substrate was sonicated for 5 min in methanol. The rinse was repeated a third time and the substrate was blown dry with a stream of nitrogen.

Film Transfer. A photoresist (AZ 5214, Clariant) layer was uniformly spin-coated onto a silicon nitride-coated wafer with a monolayer at 3,000 rpm for 30 s and baked at 110°C for 2 min. The wafer was then exposed to a 49% HF solution for 2 min. The sample was then submerged in water to release the photoresist/monolayer film from the wafer. The photoresist/monolayer film was transferred to another solid surface (i.e., Si wafer with 300-nm thermal SiO_2) by carefully dipping a solid substrate into the water and removing with photoresist/monolayer film on top. The photoresist was finally removed by sonicating in acetone for 5 min, rinsing with IPA, DI water, and drying under a stream of nitrogen, to leave only monolayer film on the new solid support.

Line and Space Patterning for Height Measurement. First, the substrate, which has a C^3M film grown on Si wafer with 300-nm SiO_2, was spin-coated with a photoresist (AZ 5214, Clariant) at 3,000 rpm for 30 s, followed by prebaking at 110°C for 2 min. Second, the substrate was aligned with a 5-μm line/space chrome mask on the MJB3 mask aligner (SUSS MicroTec) and exposed to a UV Hg lamp (365 nm) for 9 s with an intensity of 12 mW/cm^2. The substrate was then developed in a developer (AZ 327 MIF developer, Clariant) for 40 s resulting in 5-μm line/space photoresist stripes on the substrate. Next, the substrate was exposed to oxygen plasma (20 sccm O_2, 150 mTorr, 150 W) by a reactive ion-etching system (Unaxis, Plasma Thermx) for 30 s. The photoresist was finally removed by sonicating in acetone for 5 min, rinsing with IPA, DI water, and drying under a stream of nitrogen.

Contact Angle Measurements. The advancing contact angles were measured with a Ramé-Hart 100 goniometer. Contact angles were measured on six different spots of the polished side of the silicon wafer for each sample.

UV-Visible Spectroscopy. The UV-vis absorption spectra were recorded on a Shimadzu (UV-160A) spectrophotometer. The monolayers grown on a quartz slide (Chem Glass, UV-grade, 92% transmission at 270 nm) were placed in a 1-cm cuvette and the absorbance was measured by using a clean quartz slide as a background.

Fluorescence Spectroscopy. Fluorescence spectra were recorded on a Photon Technology International (QM-1) fluorometer by suspending the nonporous silicon oxide sphere with SAMs or C^3Ms in methanol (≈1 mg/ml) in a 1 cm quartz cuvette.

Secondary ion mass spectrometric measurements were carried out in a TOF-SIMS instrument (Cameca) equipped with a cesium ion gun. We measured SIMS of both SAMs and C^3Ms on their growth substrates and observed SIMS fingerprint spectra (supporting information (SI) Fig. S2) with complex correlations to the molecular weight fragments. Moreover, only small fragments (mass-to-charge ratio <400) from polymers were emitted because of chemical degradation by the high fluence of ions.

Raman Spectroscopy. The light scattered by the samples was analyzed with a Spex triplemate triple-grating monochromator (SPEX Industries) with the entrance slit set at 200 μm, a liquid-N_2-cooled CCD detector (Roper Scientific), and a data acquisition system (Photometrics). A video camera was also attached to the front port of the monochromator to facilitate laser alignment and positioning of the samples. Laser excitation (514.5 nm) was provided by an Ar ion laser (Coherent). All of the measurements were performed in ambient conditions.

Buckling Measurements of Mechanical Modulus and Structural Integrity. The modulus measurements involved several steps. First ribbons were fabricated and transferred to a prestrained slab of PDMS. Specifically, this process started with the sputter deposition of a uniform layer of Au (thickness, ≈100 nm) on a C^3M on its SiO_2/Si growth substrate. This Au layer played the role of structural support during the transfer. Next, a layer of photoresist (diluted AZ5214, 1;1 with AZ thinner, 3,000 rpm, 1min.) was spin cast on this substrate. Conformal contact of a PDMS phase mask consisting of 5 μm/5 μm line-and-space patterns, followed by flood exposure to UV light (Karl SUSS, contact aligner) for 7 s patterned the exposure of the resist, by a near-field phase-shift photolithography technique (2, 3). After removing the PDMS phase mask, the substrate was developed for 20 s in developer (AZ 327 MIF), thereby yielding ≈500-nm-wide lines of photoresist, spaced by ≈5 μm. These features of resist acted as an etch mask in an ion-milling process that removed the

exposed Au/C^3M. Oxygen plasma (PlasmaTherm) then removed the remaining photoresist. Dipping the substrate in HF undercut etched the SiO_2 and released ribbons of Au/C^3M from the substrate. A flat slab of PDMS (10:1 weight ratio of base to curing agent; Dow-Corning Sylgard 184) was used to pick up the released ribbons (still on substrate). At this stage, the ribbons were inverted, i.e., the C^3M was exposed to air while the Au layer was in contact with the PDMS. Another piece of PDMS, cured (20:1 weight ratio of base to curing agent; Dow-Corning Sylgard 184) and prestrained to 20–30%, was gently contacted and slowly peeled off of the PDMS with the ribbons of Au/C^3M, thereby transferring these ribbons to the PDMS (20:1) slab. While maintaining the prestrain, the exposed Au was removed with an Au etchant (Transcene, Inc.) and thoroughly rinsed with deionized water. Finally, the prestrain was released to induce buckling in the C^3M. The samples, before and after release of the prestrain, were characterized by atomic force microscopy, AFM (Asylum, MFD).

For the calculation of the modulus of the C^3M, the following formula (4) was used:

$$E_{C3M} = \left(\frac{\lambda}{2\pi h}\right)^3 \left[\frac{3(1-\nu_{C3M}^2)}{1-\nu_{PDMS}^2} E_{PDMS}\right],$$

where E_{PDMS} and E_{C3M} are the moduli of the PDMS and C^3M, respectively, ν_{PDMS} and ν_{C3M} are the Poisson ratios, h is the thickness of the C^3M, and λ is the buckling wavelength. Analysis by AFM indicates that λ is 630 ± 60 nm, for this system. The modulus of PDMS is ≈0.6 MPa, and its Poisson ratio is ≈0.5 (5). The value of ν_{C3M} was assumed to be 0.3. (The computed modulus depends weakly on this quantity, with only 8% change for values of ν_{C3M} between 0.3 and 0.5). The moduli extracted from this type of analysis of samples of C^3M **2** were between 1 and 10 GPa. These values are typical of polymers of similar materials. They are lower than single crystals of the of dicarbazolyl polydiacetylene (45 GPa) (6) and of graphene (≈1 TPa) (7).

Chemical Amplification. The chemical amplification process for evaluating the defect densities and barrier properties of SAMs and C^3Ms on their growth substrates consisted of: (*i*) formation of SAMs and C^3Ms on Si (100) wafers with native oxide; (*ii*) anisotropic etching of Si (KOH (52 g)/H_2O (226 ml)/IPA (74 ml), 70°C, 25 min) to convert and amplify defects in the SAMs and C^3Ms into easily imaged, micrometer-scale pits in the Si, and (*iii*) imaging the pits by optical microscopy. The Fig. 3*A Inset* image was collected after step *iii*. The process for evaluating transferred C^3Ms consisted of: (*i*) transfer of a C^3M onto a substrate of Au(200 nm)/Cr(5 nm)/SiO_2(300 nm)/Si with Au and Cr deposited by electron beam evaporation, and SiO_2 grown thermally; (*ii*) exposure of the C^3M/Au/Cr/SiO_2/Si substrate to an etchant for Au (Transene, Inc.); (*iii*) immersion in aqueous HF to remove exposed SiO_2 in the regions where the gold was removed; (*iv*) anisotropic etching of the Si (KOH (52 g)/H_2O (226 ml)/IPA (74 ml), 70°C, 25 min) to convert and amplify defects in the exposed regions into easily imaged, micrometer-scale pits in the Si; (*v*) removal of the remaining gold by aqua regia; and (*vi*) imaging the pits in the etched silicon substrate by optical microscopy. The main image in Fig. 3*A* was collected after step *ii*.

Electrical Measurements. Field effect transistor devices were used to probe the charge transport characteristics of the C^3Ms. Two types of devices were fabricated. The first used a conventional back-gate geometry with a doped Si wafer as the gate and a layer of thermally grown SiO_2 as the gate dielectric. In the first step of the fabrication of this type of device, a thin layer of isopropyl alcohol (IPA) was placed on a C^3M grown a SiO_2(300 nm)/Si substrate. A shadow mask, based on a TEM grid (Gilder Grids, 150 Mesh, Ted Pella, Inc.), was then placed on the IPA surface. Evaporation of IPA led to good physical contact of the shadow mask with the C^3M because of the action of capillary forces. Blanket electron beam evaporation (10^{-6} Torr; Temescal BJD 1800) of Ti (5 nm) and Au (50 nm) formed square-shaped contact pad arrays to define source and drain electrodes and channels with widths and lengths of 230 μm and 14 μm, respectively. Electrical measurements on C^3Ms were carried out in air by using a semiconductor parameter analyzer (Agilent 4155C), using an Agilent Metrics I/CV Lite program and a GBIP communication interface to a computer. Triaxial and coaxial shielding were used with a Signatone probe station to yield high signal-to-noise ratio measurements of small current levels. Measurements on these devices at room temperature reveal the resistivities on the order of 10^5-10^6 Ω·cm, independent of gate bias.

The second type of transistor device used polymer electrolyte gating. In this case, source and drain electrodes were patterned in the same geometries and with the same techniques as those used for the conventional devices described earlier. A solution 30% 1:3 (w:w) $LiClO_4$:polyethyleneimine in methanol was used as the polymer electrolyte. The electrolyte was placed in a poly-(dimethylsiloxane) fluidic channel formed with a piece of molded PDMS on top of a C^3M. A silver wire immersed in the electrolyte was used to apply gate voltages between −0.5 V and 0.5 V. The bias between the source and drain electrodes was 0.1 V. The measured source-drain currents were smaller than ≈10 nA, comparable to the gate leakage in these devices. The conclusions from these measurements are consistent with those from devices with the more conventional back-gate device geometry.

Preparation of Substrate with Patterned Holes. A substrate with patterned holes was prepared by using Solvent Assisted Micro-Molding (SAMIM) (8). First, a film of epoxy with the thickness of ≈10 μm (NanoSU-8, MicroChem, formulation 10) was deposited onto a glass slide by spin coating at 3,000 rpm for 30 s, followed by soft-baking at 65°C and 95°C for 1 min and 5 min, respectively. Second, the quasi-3D type of mold made of acryloxy perfluoropolyether (a-PFPE) was wetted with ethanol and gently placed into conformal contact on soft-baked substrate from the first step for 30 min. The mold was then peeled off from the substrate followed by exposure of the substrate to a UV Hg lamp (365 nm) from an MJB3 mask aligner (SUSS MicroTec) for 30 s with an intensity of 12 mW/cm^2 and rebaked at 65°C and 95°C for 1 min and 5 min, respectively. Finally, the substrate was hard-baked at 180°C for 5 min and coated with thin films of Ti/Au (2 nm/ 50 nm) by an electron beam evaporation system (Temescal).

Preparation of Smoothed Patterned Substrate. The procedure above was followed except the SU-8 was spin-coated on a silicon wafer. The steps were smoothed by exposure to thermal flow at 60°C for 6 min after peeling off the mold and before UV exposure. This smoothing resulted in a decrease of the steps from 350 nm to 35 nm and the sharp edges became sloped (Fig. S5). Finally, a 50-nm silicon oxide film was deposited onto the plasmonic crystal using PECVD instead of coating with Ti/Au films. SF5

High-resolution Microscopic Characterizations of C^3M 1. The STM image (Fig. S6*A*) was obtained by transferring C^3M **1** onto a freshly cleaved highly oriented pyrolytic graphite surface. Although certain insights can be obtained from such images, molecular scale detail was difficult to obtain. We believe that residue associated with manipulation and synthesis of the C^3M represent the main challenge to achieving molecular resolution (9). As an alternative, we conducted ultra-high-resolution AFM SF6

SF6 measurements with AFM tips that have radii of curvature as small as 2 nm. Fig. S6*B* shows a typical result. The rms roughness of C^3M **1** is 0.17 nm, nearly identical to that of the bare SiO_2 growth surface. No filamentary structures were visible. For a final set of data, we performed high-resolution TEM on transferred C^3M **1** under low-dose conditions. Images (Fig, S6*C*) show what appear to be strands of polymers separated by a distance of ≈3.35 Å, which might provide direct information on the possibility of woven-network structures. These features may, however, be caused by even slight damage induced by exposure to the electron beam.

SF6

XPS Spectroscopy for Characterization of Metal Content. XPS spectroscopy was used to determine whether metal remains on the surface after the Mo(IV) catalyzed linkage of a SAM of **1**. We found the doublet for Mo($3d_{5/2}$) and Mo($3d_{3/2}$) at 226 and 239 eV, corresponding well to the literature data for Mo (10). A strong C(1s) peak appeared at 283 eV. Integration of the XPS peaks for Mo and C generated a molybdenum-to-carbon ratio of 1.45% at the surface. Quantitative analysis of trace amount of Cu catalysts in linked SAMs from **2** and **3** was difficult because of the low kinetic energy the photoelectrons.

1. Zhang W, Kraft S, Moore JS (2004) Highly active trialkoxymolybdenum(VI) alkylidyne catalysts synthesized by a reductive recycle strategy. *J Am Chem Soc* 126:329–335.
2. Rogers JA, Paul KE, Jackman RJ, Whitesides GM (1997) ●●● *Appl Phys Lett* 70:2658.
3. Maria J, Malyarchuk V, White J, Rogers JA (2006) ●●● *J Vacuum Sci Technol B* 24:828.
4. Khang DY, Jiang H, Huang Y, Rogers JA (2006) A stretchable form of single-crystal silicon for high-performance electronics on rubber substrates. *Science* 311:208–212.
5. Wilder EA, Guo S, Lin-Gibson S, Fasolka MJ, Stafford CM (2006) ●●●. *Macromolecules* 39:4138.
6. Galiotis C, *et al.* (1984) ●●●. *J Polym Sci Polym Phys Ed* 22:1589.
7. Bunch JS, *et al.* (2007) Electromechanical resonators from graphene sheets. *Science* 315:490–493.
8. Truong TT, *et al.* (2007) Soft lithography using acryloxy perfluoropolyether composite stamps. *Langmuir* 23:2898–2905.
9. Ishigami M, Chen JH, Cullen WG, Fuhrer MS, Williams ED (2007) Atomic structure of graphene on SiO_2. *Nano Lett* 7:1643–1648.
10. Solymosi F, Cserényi J, Szöke A, Bánsági T, Oszkó A (1997) ●●●. *J Catal* 165:150–161.

AQ: A AQ: B AQ: C AQ: D AQ: E

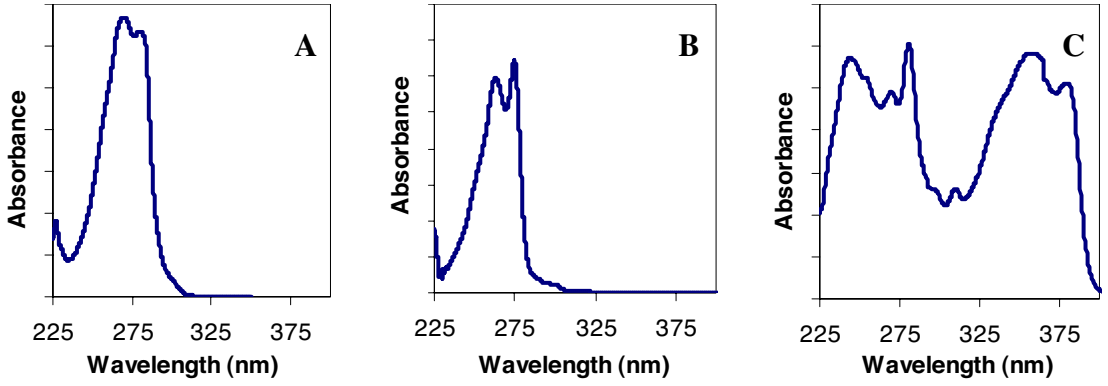

Fig. S1. UV-vis spectra of monomers in dichloromethane. (*A*) Dipropyne monomer 1. (*B*) Diacetylene monomer 2. (*C*) Terphenyl monomer 3.

SF1

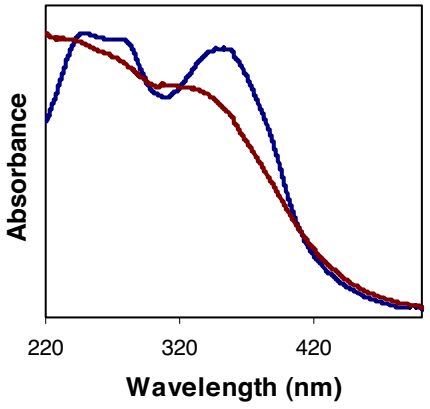

Fig. S2. UV-vis spectra of a SAM of 3 (blue) and linked SAM from 3 (red) on quartz.

SF2

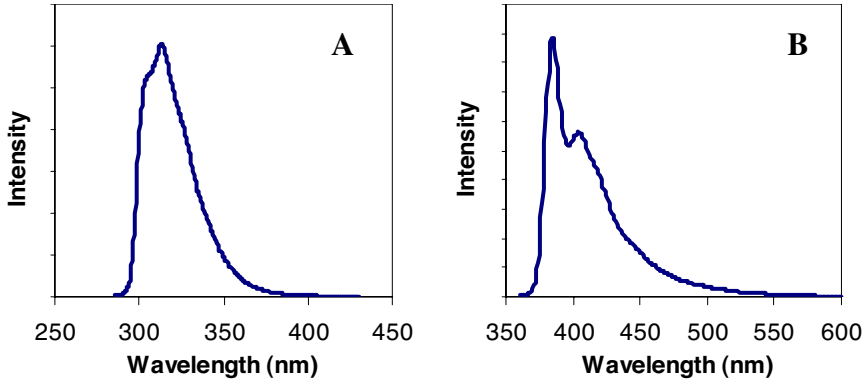

Fig. S3. Fluorescence spectra of monomers in methanol. (*A*) Diacetylene monomer 2 excited at 275 nm. (*B*) Terphenyl monomer 3 excited at 350 nm.

SF3

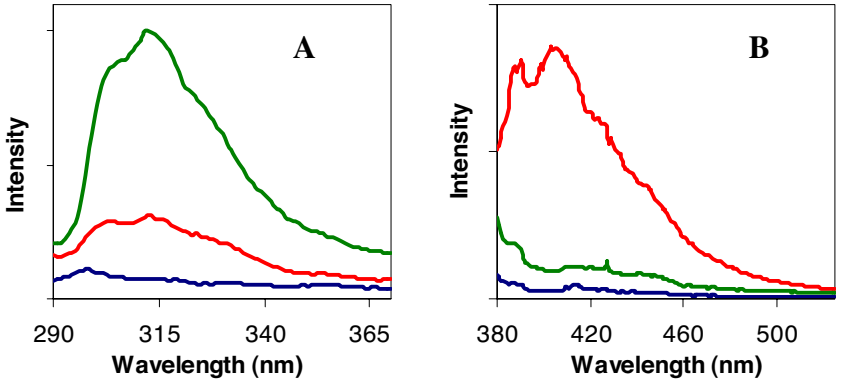

Fig. S4. Combined fluorescence spectra for SAMs and linked SAM from **2** on SiO_2 spheres suspended in methanol. (*A*) Fluorescence from excitation at 275 nm. Bare SiO_2 spheres (blue), SAM from **2** (green) linked SAM from **2** (red). (*B*) Fluorescence from excitation at 370 nm. Bare SiO_2 spheres (blue), SAM from **2** (green), linked SAM from **2** (red). Peak heights were normalized to the 315-nm emission of the SAM from **2**.

SF4

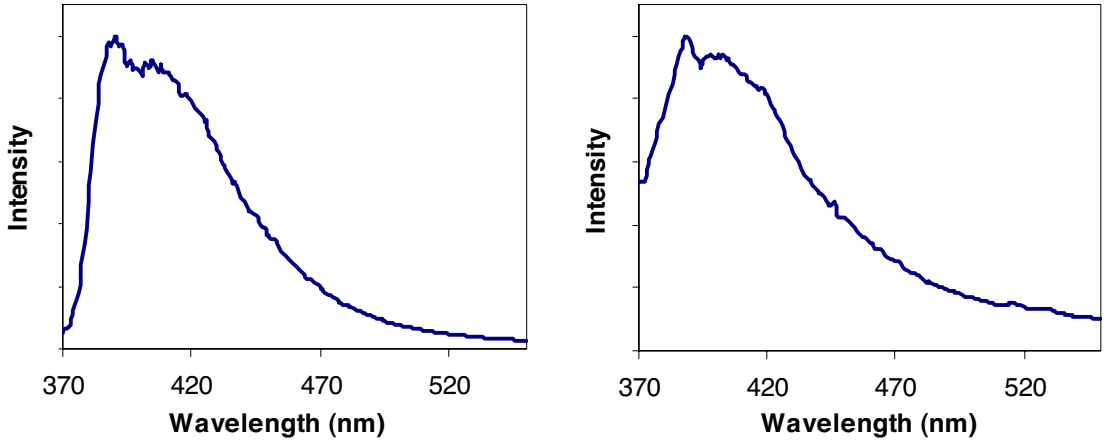

Fig. S5. Fluorescence spectra of SAMs and C^3M from **3**. (*A*) Fluorescence spectrum for SAM from **3** on SiO_2 spheres at 350-nm excitation. (*B*) Fluorescence spectrum for linked SAM from **3** on SiO_2 spheres at 350-nm excitation

SF5

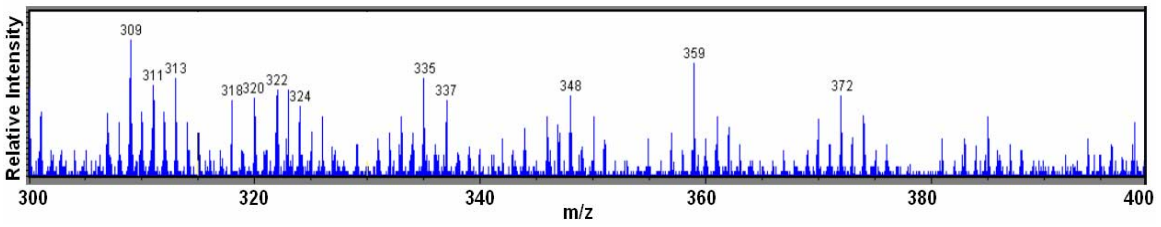

Fig. S6. A representative secondary ion mass spectrum of linked SAM from **2** on its growth substrate (Si wafer with 300-nm thermal SiO_2).

SF6

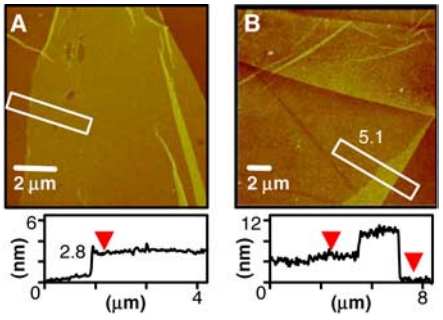

Fig. S7. Source drain current-gate voltage characteristics of a representative back-gate-linked SAM from **2** device (*A*) and polymer electrolyte gate-linked SAM from **2** device (*B*). *Insets* show schematic illustrations of cross section and optical image of device.

SF7

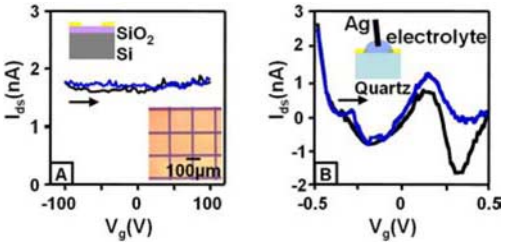

Fig. S8. AFM images of linked SAMs. (*A*) AFM image and step height of a linked SAM from **2** transferred to a flat Si wafer with 300-nm thermal SiO_2. The graph shows an averaged line cut, revealing a step height of ≈2.8 nm. (*B*) AFM image and step height of a linked SAM from from **3** transferred to a flat Si wafer with 300-nm thermal SiO_2. The graph shows an averaged line cut, revealing a step height of ≈5.1 nm.

SF8

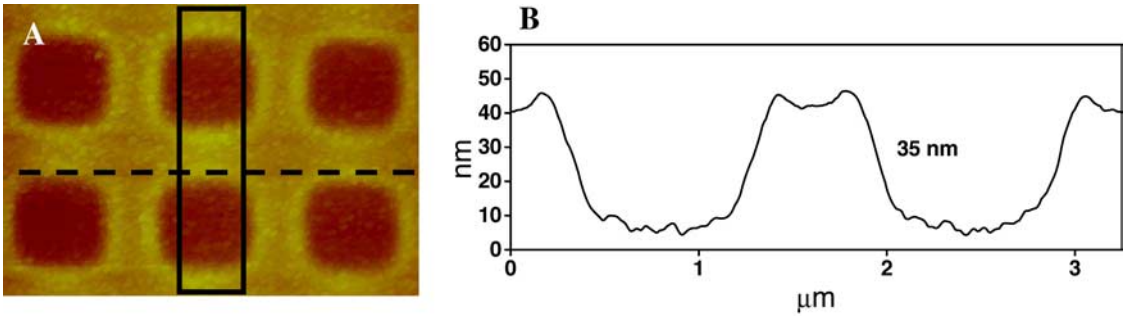

Fig. S9. Atomic force microscope (AFM) characterization of structured growth substrate. (*A*) Tapping mode AFM image of patterned substrate. (*B*) An averaged line cut from *A*, revealing a relief depth of 35 nm.

SF9

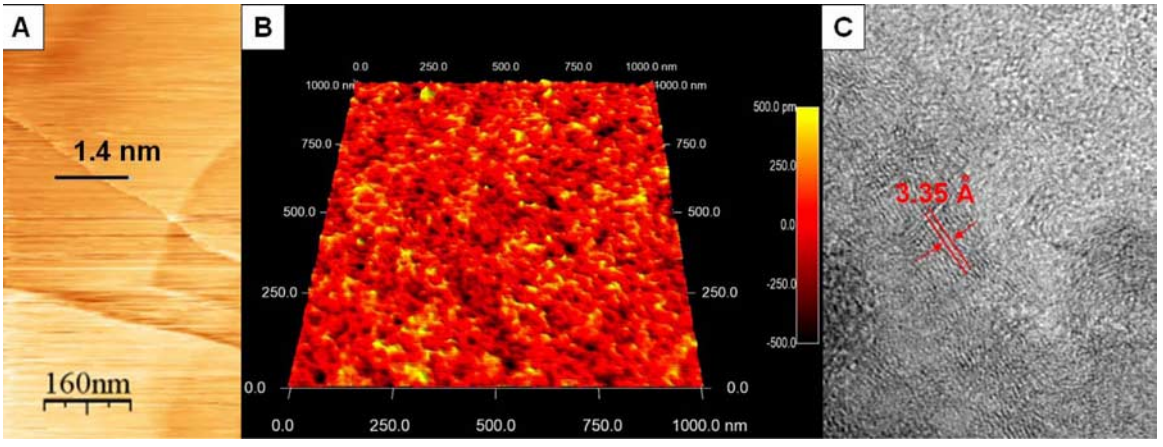

AQ: F **Fig. S10.** ●●●. (*A*) A STM image of transferred linked SAM from **1** on a freshly cleaved, highly oriented pyrolytic graphite surface. The cross-sectional height is ≈1.4 nm. (*B*) An AFM image of linked SAM from **1** on the growth substrate (Si wafer with 300-nm thermal oxide). The AFM tip radius = 2 nm. The rms of C^3M **1** is 0.17 nm, nearly identical to that of bare SiO_2 surface. (*C*) A TEM image of transferred linked SAM from **1** on a holey carbon TEM grid under a low-dose condition, showing what appear to be strands of polymers separated by a distance of ≈3.35 Å.

SF10

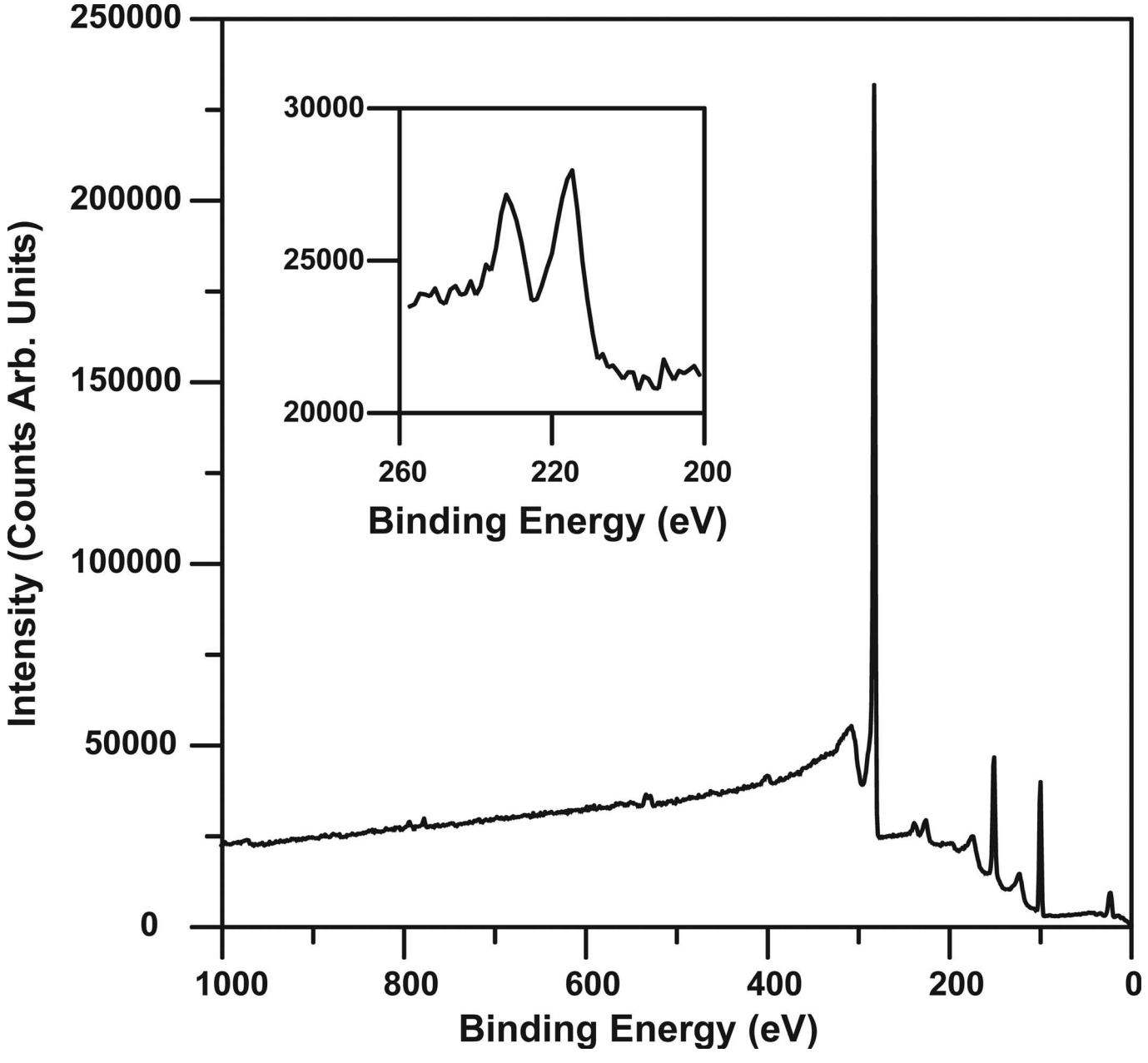

Fig. S11. XPS spectra of a C^3M **1** on a Si wafer with a 300-nm thermal SiO_2 layer. *Inset* shows Mo 3d peaks.

Sf11

Table S1. Contact angle measurements for SAMs and linked SAM from 1, 2, and 3 on SiO_2, silicon nitride, and quartz wafers

Support	SAM **1**	Linked SAM **1**	SAM **2**	Linked SAM **2**	SAM **3**	Linked SAM **3**
Silicon oxide	74 (1)	69 (2)	75 (1)	64 (2)	80 (1)	59 (1)
Silicon nitride	74 (2)	70 (2)	77 (1)	64 (2)	80 (1)	62 (1)
Quartz	74 (2)	69 (1)	76 (2)	65 (3)	86 (2)	56 (3)

ST1

AUTHOR QUERIES

AUTHOR PLEASE ANSWER ALL QUERIES 1

A—Au: Please supply article title and last page in page range, if this article is longer than one page.

B—Au: Please supply article title and last page in page range, if this article is longer than one page.

C—Au: Please supply article title and last page in page range, if this article is longer than one page.

D—Au: Please supply article title and last page in page range, if this article is longer than one page.

E—Au: Please provide article title.

F—Au: Please supply a short, general heading to describe figure as a whole, before discussing parts of the figure.

PNAS
Proceedings of the National Academy of Sciences of the United States of America www.pnas.org

2008 Reprint and Publication Charges

Reprint orders and prepayments must be received no later than 2 weeks after return of your page proofs.

PUBLICATION FEES

Page Charges
(Research Articles Only)

Page charges of $70 per journal page are requested for each page in the article. PNAS charges for extensive author alterations on proofs. Six or more author alterations per page will be charged at $4 each. Authors will not be charged for correcting printer's errors, copyediting errors, or figure errors made in composition.

Articles Published with Figures
(Research Articles Only)

If your article contains color, add $325 for each color figure or table. Replacing, deleting, or resizing color will cost $150 per figure or table. Replacing black-and-white figures will cost $25 per figure. State the exact figure charge on the following page and add to your payment or purchase order accordingly.

Supporting Information
(Research Articles Only)

Supporting information for the web will cost $250 per article.

PNAS Open Access Option

Authors may pay a surcharge of $1200 to make their paper freely available online immediately upon publication. If your institution has a 2008 Site License, the open access surcharge is $850. If you wish to choose this option, please notify the Editorial Office (pnas@nas.edu) immediately, if you have not already done so.

Shipping

UPS ground shipping within the continental U.S. (1–5 days delivery) is included in the reprint prices, except for orders over 1,000 copies. Orders are shipped to authors outside the continental U.S. via expedited delivery service (included in the reprint prices).

Multiple Shipments

You may request that your order be shipped to more than one location. Please add $45 for each additional address.

Delivery

Your order will be shipped within 2 weeks of the journal publication date.

Tax Due

For orders shipped to the following locations, please add the appropriate sales tax:

Canada – 6%; in the U.S.: CA – 7.25% plus the county rate; CT – 6%; DC – 5.75%; FL – 6% sales tax plus local surtax, if you are in a taxing county; MD – 5%; NC – 4.5%; NY – state and local sales taxes apply; VA – 5%; WI – 5%. A copy of the state sales tax exemption certificate must accompany the order form; otherwise, sales tax will be assessed (billed).

Ordering

Prepayment or a signed institutional purchase order is required to process your order. You may use the following page as a Proforma Invoice. Please return your order form, purchase order, and payment to:

PNAS Reprints
PO Box 631694
Baltimore, MD 21263-1694
FEIN 53-0196932

Please contact Robin Wheeler by e-mail at wheelerr@cadmus.com, phone 1-800-407-9190 (toll free) or 1-410-819-3903, or fax 1-410-820-9765 if you have any questions.

Covers are an additional $75 regardless of the reprint quantity ordered. Please see reprint rates and cover image samples below.

Rates for Black-and-White Reprints* (Minimum order 50. Includes shipping.)

Quantity	50	100	200	300	400	500	Add'l 50s over 500
Domestic	$440	$595	$620	$675	$730	$775	$55
Foreign	$475	$630	$685	$775	$850	$920	$75

*** Color covers may be ordered for black-and-white reprints; however, color reprint rates (below) will apply.**

For Black-and-White and Color Reprint Covers add $75

Rates for Color Reprints† (Minimum order 50. Includes shipping.)

Quantity	50	100	200	300	400	500	Add'l 50s over 500
Domestic	$490	$615	$825	$1,110	$1,425	$1,740	$160
Foreign	$550	$665	$885	$1,200	$1,575	$2,015	$215

†Please return your order form promptly.

Covers for black-and-white reprints will display the volume, issue, page numbers, and black-and-white PNAS masthead with the reprint article title and authors imprinted in the center of the page.‡

Covers for color reprints will display the volume, issue, page numbers, and the color PNAS masthead and will include the issue cover image with the reprint article title and authors imprinted in the center of the page.‡

‡Covers for all reprints will be printed on the same paper stock as the article.

PNAS
Proceedings of the National Academy of Sciences of the United States of America www.pnas.org

2008 Reprint Order Form or Proforma Invoice

(Please keep a copy of this document for your records.)

Reprint orders and payments must be received no later than 2 weeks after return of your proofs.

1 Publication Details

Reprint Order Number 3350389

Author's Name _____

Title of Article _____

_____

Number of Pages _____ Manuscript Number 07-10081

Are there color figures in the article? ❑ Yes ❑ No

2 Reprint Charges (Use Rates Listed on Previous Page)

Indicate the number of reprints ordered and the total due. Minimum order is 50 copies; prices include shipping.

Research, Special Feature Research, From the Academy, and Colloquium Articles:

_____ Reprints (black/white only) $ _____

_____ Color Reprints (with or without color figures) $ _____

_____ Covers $ _____

For Commentary, Inaugural, Solicited Review, and Solicited Perspective Articles Only:

_____ First 100 Reprints (free; black/white or color)

_____ Covers $ _____

Subtotal $ _____

Sales Tax* $ _____

Total $ _____

*For orders shipped to the following locations, please add the appropriate sales tax: Canada – 6%; in the U.S.: CA – 7.25% plus the county rate; CT – 6%; DC – 5.75%; FL – 6% sales tax plus local surtax, if you are in a taxing county; MD – 5%; NC – 4.5%; NY – state and local sales tax apply; VA – 5%; WI – 5%. A copy of the state sales tax exemption certificate must accompany the order form; otherwise, sales tax will be assessed (billed).

3 Publication Fees (Research Articles Only)

Pages in article @ $70 per page requested $ _____

Color figures or tables in article @ $325 each $ _____

Replacement or deletion of color figures @ $150 each $ _____

Replacement of black/white figures @ $25 each $ _____

Supporting information @ $250 per article $ _____

Open Access option @ $1200 ($850 if your institution has a 2008 Site License/Open Access Membership) per article $ _____

Subtotal $ _____

TOTAL AMOUNT due for reprint and publication fees $ _____

4 Invoice Address It is PNAS policy to issue one invoice per order.

Name _____

Institution _____

Department _____

Address _____

City _____ State _____ Zip _____

Country _____

Phone _____ Fax _____

Purchase Order Number _____

5 Shipping Address (if different from Invoice Address)

Name _____

Institution _____

Department _____

Address _____

City _____ State _____ Zip _____

Country _____

Quantity of Reprints _____

Phone _____ Fax _____

6 Additional Shipping Address †

Name _____

Institution _____

Department _____

Address _____

City _____ State _____ Zip _____

Country _____

Quantity of Reprints _____

Phone _____ Fax _____

†Add $45 for each additional shipping address.

7 Method of Payment

❑ Credit Card ❑ Personal Check (enclosed) ❑ Institutional Purchase Order (enclosed)

8 Credit Card Payment Details

Total Due _____

❑ Visa ❑ MasterCard ❑ AMEX

Card Number _____

Exp. Date _____

Signature _____

9 Payment Authorization

❑ I assume responsibility for payment of these charges.
(Signature is required. By signing this form, the author agrees to accept responsibility for payment of all charges described in this document.)

_____
Signature of Responsible Author

_____
Phone Fax

3350389 07-10081

Reprint Order Number Manuscript Number

Send payment and order form to **PNAS Reprints**, PO Box 631694, Baltimore, MD 21263-1694 FEIN 53-0196932
Please e-mail wheelerr@cadmus.com, call 1-800-407-9190 (toll free) or 1-410-819-3903, or fax 1-410-820-9765 if you have any questions.

Instructions for Annotating Your .PDF Proof

- Use Text Boxes and the Callout Tool to indicate changes to the text.

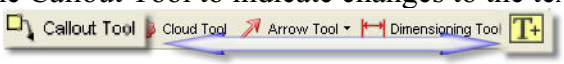

- Use the Strike-Out tool to indicate deletions to the text.

- Use the Highlighting Tool to indicate font problems, bad breaks, and other textual inconsistencies.

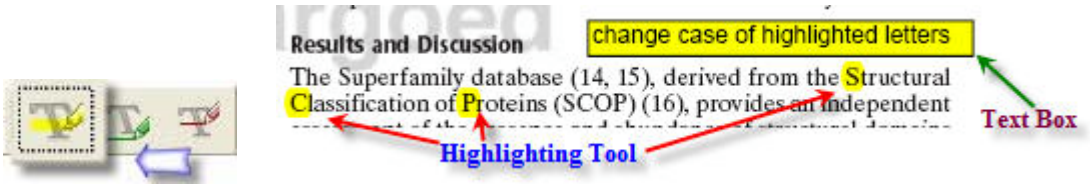

- Clearly indicate where changes need to be made using arrow, lines, and the Call-Out Tool.

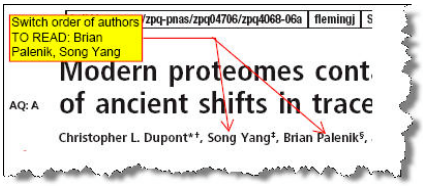

- Mark changes and answer queries in the margins and other areas of white space.

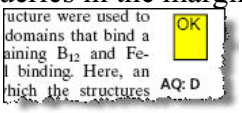

- Avoid obscuring the text with corrections.

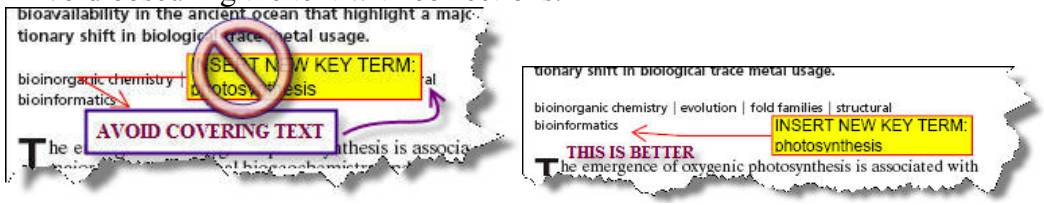

Proofreader's Marks

MARK	EXPLANATION	EXAMPLE
	TAKE OUT CHARACTER INDICATED	 Your proof.
	LEFT OUT, INSERT	 Your proof.
	INSERT SPACE	 Yourproof.
	TURN INVERTED LETTER	Your proof.
	BROKEN LETTER	Your proof.
	EVEN SPACE	A good proof.
	CLOSE UP: NO SPACE	Your proof.
	TRANSPOSE	A proof good
	WRONG FONT	 Your proof.
	LOWER CASE	Your proof.
	CAPITALS	Your proof.  Your proof.
	ITALIC	Your proof. Your proof.
	ROMAN, NON ITALIC	 Your proof.
	BOLD FACE	Your proof. Your proof.
	LET IT STAND	Your proof.  Your proof.
	DELETE, SEE COPY	She Our proof.
	SPELL OUT	 Queen Eliz.
	START PARAGRAPH	 read. Your
	NO PARAGRAPH: RUN IN	marked. Your proof.
	LOWER	 Your proof.

MARK	EXPLANATION	EXAMPLE
	RAISE	 Your proof.
	MOVE LEFT	Your proof.
	MOVE RIGHT	Your proof.
	ALIGN TYPE	Three dogs. Two horses.
	STRAIGHTEN LINE	Your proof.
	INSERT PERIOD	Your proof
	INSERT COMMA	Your proof
	INSERT COLON	Your proof
	INSERT SEMICOLON	Your proof
	INSERT APOSTROPHE	Your mans proof.
	INSERT QUOTATION MARKS	Marked it proof
	INSERT HYPHEN	A proofmark.
	INSERT EXCLAMATION MARK	Prove it
	INSERT QUESTION MARK	Is it right
	QUERY FOR AUTHOR	Your proof read by
	INSERT BRACKETS	The Smith girl
	INSERT PARENTHESES	Your proof 1
	INSERT 1-EM DASH	Your proof.
	INDENT 1 EM	Your proof
	INDENT 2 EMS	Your proof.
	INDENT 3 EMS	Your proof.